This study's object is the stressed state of the plastic deformation site under conditions of load asymmetry when metal is gripped by rolls, under the determining modes of process stability. The task addressed is the implementation of shape change at the rolling process stability threshold related to a decreased force load under the increased strain impact.

A physical and mathematical model of a flat rolling theory problem has been built under conditions of multi-parameter factors affecting the gripping capacity of rolls and the stability of rolling process.

The plasticity theory problem was solved analytically using the method of argument of a function of a complex variable. The solution to the plane problem is shown, using the asymmetry of the process, the counter-directed flow of metal. The nonlinearity of the plasticity theory problem was taken into account.

Based on the mathematical model, a new force factor was identified and investigated: the force stretching factor from the lagging zone. A new single-zone deformation mode with minimum process stability was identified. The process was investigated under conditions of multiparameter influence on rolls gripping ability and its stability. The zones of reachability were established for a deformation focus shape factor within the range of 5.00...15.00. The mode of partial suppression of the zeroing factors of the metal stressed state was investigated under conditions of multi-parameter influence on the gripping ability of the rolls and the stability of the process. Stability indicators of transient modes were determined: at $\alpha = 0.077$, the ratio $f/\alpha = 1.10...1.95$; at $\alpha = 0.129$, the ratio $f/\alpha = 1.19...1.95$; at $\alpha = 0.168$, the ratio $f/\alpha = 1.28...1.95$.

This study's results make it possible to solve technological problem related to the development of rolling schemes when the gripping force of friction and the pushing force of normal pressure arise during the forming process

Keywords: loading asymmetry, counter-directed metal flow, loss of stability, stressed-strained state

UDC 539.3

DOI: 10.15587/1729-4061.2025.340835

IDENTIFYING A MECHANISM FOR THE GRIPPING ABILITY OF ROLLS AND ROLLING AT A STABILITY LIMIT UNDER ASYMMETRIC LOADING

Valeriy Chigirinsky
Doctor of Technical Sciences, Professor*
Abdrakhman Naizabekov
Doctor of Technical Sciences, Professor*
Sergey Lezhnev
Candidate of Technical Sciences, Professor*
Olena Naumenko
Corresponding author
Senior Lecturer
Department of Mechanical and Biomedical Engineering
Dnipro University of Technology
Dmytra Yavornytskoho ave., 19, Dnipro, Ukraine, 49005
E-mail: naumenko.o.h@nmu.one
Sergey Kuzmin
Candidate of Technical Sciences*
Sergey Melentyev
Senior Lecturer*
*Department of Metallurgy and Mining
Rudny Industrial Institute
50 Let Oktyabrya str., 38,
Rudny, Republic of Kazakhstan, 111500

Received 19.06.2025
Received in revised form 11.09.2025
Accepted 22.09.2025
Published 30.10.2025

How to Cite: *Chigirinsky, V., Naizabekov, A., Lezhnev, S., Naumenko, O., Kuzmin, S., Melentyev, S. (2025). Identifying a mechanism for the gripping ability of rolls and rolling at a stability limit under asymmetric loading. Eastern-European Journal of Enterprise Technologies, 5 (1 (137)), 31–54. https://doi.org/10.15587/1729-4061.2025.340835*

1. Introduction

With the rapid development of technology, the boundary conditions of many applied problems are becoming more complex, necessitating the expansion and sophistication of process models, identifying not the solutions themselves but the conditions for their existence and generalizations.

The nonlinearity of plasticity theory problems, including boundary conditions, as well as the complexity of their analytical solution and generalization are a challenge.

Practical experience shows that achieving the ultimate deformation zone effect during plastic forming depends on the gripping ability of the rolls and the conditions for achieving a stable rolling process.

It is very difficult to reconcile the obtained results for stresses and strains (strain rates). Experience shows that solutions lose their relevance because of the failure to consider lost models and the adoption of unjustified simplifications.

Such a complex structure of the identified effect is explained by its multi-parameter impact and the complexity of loading different zones of the deformation site.

It becomes necessary to characterize the gripping ability of rolls and the rolling process stability using more than one indicator. The need to revise the conditions for roll gripping and process stability loss stems from the fact that existing developments on roll gripping are insufficient and fail to explain many theoretical and practical aspects of the process.

Therefore, research into the mechanics of interaction between multiparameter factors on roll gripping and rolling process stability, along with the construction of a mathematical model, is urgently needed. Furthermore, technological advancements that encompass a wide range of areas in solid

mechanics, in various states and address various applied problems, are of interest.

2. Literature review and problem statement

In [1], the contradictory effects of plastic forming were considered; the effect of decreasing force loading with increasing deformation was identified and studied. However, the implementation of this effect remained unclear. The reasons are the lack of data on force loading during metal gripping by rolls and the absence of force characteristics for process stability loss. The relevance of the problem also relates to the fact that such effects can fundamentally change rolling production technologies. Reducing the rolling force with increasing deformation loading allows for the following: decreasing the spring rate of the mechanical system; rolling tolerances; increasing the yield due to minus rolling; reducing roll wear; and increasing mill productivity. Advances in thermomechanical processing of metal in the mill flow will improve the metal structure and its phase composition, improve the quality of rolled products, as well as reduce their cost.

An indicator of the reliability of result is the possibility of generalizing the approaches of a method, in particular the method of argument functions of a complex variable, to other areas of mechanics. This enhances its significance in solving applied and general theoretical problems. The fundamentals of the method were outlined in [1–7].

The method was used to consider problems in [1, 2], under fundamentally different loading of zones in the plastic deformation site. The combined influence of various factors on the process was demonstrated, including the friction coefficient, the grip angle, and the deformation site shape factor. However, the mechanism for implementing this process was not specified in those studies, which precludes its use in further analysis and application.

The first attempts to formulate specific provisions of the argument-function method were published in [3]. The method was further developed in [4], in which it was not specific theoretical questions that were formulated but general approaches that allow for the use of the invariance of differential relations in continuum mechanics. Based on the invariance of transformations, papers were published for problems in elasticity theory [4, 5], plasticity theory [6], and problems of dynamic processes. At the fundamental level, practical issues of geomechanics [7], beam loading mechanics with complex boundary conditions and in different reference frames [5], and the wave theory of dynamic problems [4] with applications to rotational vibrations in the main line of a rolling mill were considered. The capabilities of the method allow for an expansion of the scope of application of the obtained solutions through generalized approaches, including the Cauchy-Riemann relations and the Laplace equations, which allow for the closure of solutions to problems in continuum mechanics.

The validity of theoretical problem solutions is significantly confirmed when the results correspond to general trends in the development of science and technology [8]. The methodology described in [8] takes into account the influence of horizontal loading on the force state of the specimen. It is substantiated by the distribution of standard contact stresses arising from shear stresses and stresses generated by contact friction. However, issues related to the interaction of areas with different force loading remain unresolved. This may be due to the lack of an adequate physical model of the loading process.

The boundary conditions of many applied problems are becoming more complex, necessitating the expansion and sophistication of process models, finding not the solutions themselves but the conditions for their existence and generalizations. In this regard, an important factor is the response of the literature to the problem of generalizations in theory and practice [9]. The work lacks an applied section that would allow for the implementation of the intended generalizations, which precludes its practical application.

The mathematical theory of plasticity is based on specific ideas, encompassing a range of applied problems and allowing for the generalization of these solutions using approaches inaccessible to other frameworks [10]. In this case, the challenge is the nonlinearity of plasticity theory problems and the complexity of their analytical solution and generalization. A possible solution to these problems is closed-loop plasticity theory problems, both in terms of stress and strain rates, which can address problems with complex boundary conditions. In this case, there is evidence not of a virtual stressed-strained state of the plastic medium but of an actual one. As analysis reveals, the possibility arises of complicating the solution to such problems, i.e., taking into account the multicomponent nature of the impact and response.

The greatest difficulty in solving problems in plasticity theory pertains to spatial problems [11], particularly if the statement and solution consider a closed problem, making it difficult to reconcile the obtained results in terms of stresses and strains (strain rates). Experience shows that simplified solutions cannot be used as they fail to account for the influence of lost models and the adoption of unjustified simplifications. The unjustified nature of simplifications manifests itself in solutions to plasticity problems involving only stresses or only strains, including variational principles of mechanics, where the functionality varies only in terms of strains or only stresses. This loses the multifactorial nature of the approach, neglecting the influence of factors on process parameters, such as the stretching of the lagging zone on the gripping ability of the rolls and the stability of the rolling process.

In [12], metal loading under strain is studied. However, loading can be considered somewhat more broadly, for example, asymmetric and symmetric ones, which expands the range of problems to be solved. Asymmetric processes pose difficulties in satisfying complex boundary conditions. However, it is possible to characterize processes using physical and mathematical models, examining the influence of loading asymmetry on process stability, or to consider processes on the verge of loss of stability, where complex plastic deformation effects are possible.

When stating problems in mechanics, systems of equations are considered that can be categorized as equations of mathematical physics. These primarily include hyperbolic, elliptic, and parabolic partial differential equations. The greatest degree of generalization of solutions is considered in mathematical physics. These include methods such as separation of variables, characteristics, Riemann, Fourier, d'Alembert, integral transformations, and others [13]. However, issues of interaction within a single deformation site have not been adequately addressed, preventing consideration of certain features of force loading.

Many solutions within plasticity and elasticity theory utilize the stress function method [14], which yields reliable results (it can be effectively used, with certain simplifications, as a test of the theory of argument functions of a complex variable). However, these solutions relied on assumptions that prevented

characterization of certain loading features of the deformation site. For example, the solution for loading a wedge-shaped half-space with a concentrated force did not account for the influence of shear stresses on the lateral surface due to the impossibility of satisfying the boundary conditions. Paper [7] reported a solution to overcome the difficulties associated with boundary conditions for shear stresses. This solution demonstrated schemes in which shear stresses had large magnitudes and normal stresses changed sign to the opposite. Thus, simplified loading ignored dangerous normal tensile stresses and increased shear effects.

In [15], discrepancies between the stress and strain states of a plastic medium due to field mismatches were demonstrated. Solutions are presented that allow one to resolve contradictions between theoretical and experimental data, using the identified effects of twisting of conjugate slip planes. These approaches are productive, as they allow one to conceptualize the process of plastic deformation as close to a closed problem in plasticity theory. Furthermore, processes involving effects involving multidirectional metal flow during rolling can be re-evaluated, yielding not only theoretical but also practical results.

In [16], cyclic loading is demonstrated for the case of simple shear, which elicits a corresponding response from internal stresses. A basic trigonometric function is introduced into the analysis. The loading capabilities for varying boundary conditions, including the trigonometric function, are presented, but there is no correspondence between it and other basic dependences, such as exponential functions, which are capable of closing the solution in combination with the application option proposed in the paper.

In [17], an example of using a function argument using a coordinate reference system is given, which significantly expands the solution's capabilities. These can subsequently be used as closing functions for the problem being solved.

In [18], loading of a foundation with a specific discontinuity was studied. The stressed state heterogeneity was characterized by trigonometric and exponential expressions. The proposed combination of functions allows for an expansion of their applicability by simplifying boundary conditions and assessing the interaction of differently loaded areas of the deformation site.

A solution is demonstrated using a fundamental substitution [19], which can be a basic function in solving a closed-loop problem in plasticity theory. However, this is insufficient to characterize the interaction of differently loaded zones of the deformation site: a combination with a trigonometric function must be considered.

In [20], the use of an exponential function in the solution is demonstrated, confirming the relevance of its application in problems of continuum mechanics. The exponent can play a role as the second argument of the function when solving a closed-loop problem in plasticity theory. However, as analysis has revealed, without the first argument of the function, the closed-loop problem cannot be solved. The reason for this discrepancy may be the lack of a necessary physical model of the deformation process.

In [21], differential relations for the transition from one variable to another are used, which characterize certain generalizations and simplifications when solving analytical problems in plasticity theory. Such approaches are acceptable for problems in continuum mechanics. However, invariant differential relations between variables in the form of Cauchy-Riemann relations, which unambiguously determine the conditions for the existence of solutions to a closed problem in plasticity theory, are absent. This is due to the lack of a physical model of the process under asymmetric loading.

In [22], the boundary conditions of the problem are mathematically justified using the collocation method. Their determination is a problem in continuum mechanics. However, issues of nonlinearity of the boundary conditions remain undefined, preventing the identification of transformation options for the solutions themselves. This may be due to the inability to adequately state the physical and mathematical problem of continuum mechanics.

In conclusion, it should be noted that the literature addresses the issue of solving problems with elements of generalizations of complex problems in continuum mechanics. Furthermore, questions arise when posing and solving complex physical and mathematical problems determined by modern advancements in engineering and technology, particularly in rolling processes. The use of the characteristics and patterns of plastic deformation in the development of fundamental innovative advancements in manufacturing is of interest. The literature contains studies identifying the effects of plastic deformation associated with a reduction in force loading under conditions of increasing deformation effects to the point of process instability. However, the technological conditions and mechanisms that the instability process and the entire rolling process must comply with are unknown. All of this suggests that it is advisable to study the mechanism of roll gripping and rolling at the point of process instability when the effect of plastic deformation is realized.

3. The aim and objectives of the study

The objective of our study is to determine the mechanism of roll gripping ability and rolling at the limit of process stability under conditions of asymmetric loading on the plastic deformation site. This will enable the realization of the effect of plastic shape change under an asymmetrically loaded deformation site.

To achieve this aim, the following objectives were accomplished:

– to build a physical and mathematical model of a plane rolling theory problem under conditions of multiparameter factors influencing roll gripping ability and rolling stability;

– based on the resulting mathematical model, to identify, study, and analyze the process of minimum stability and the process of suppressing the effect on the zeroing factors of the stressed state under conditions of multiparameter loading during metal gripping by rolls, as well as stability in the zone of attainability of the limiting deformation site;

– to evaluate the reliability of would-be results from our study on the stressed state of metal under the influence of multiparameter factors on gripping and rolling stability, including finite element modeling in the DEFORM program.

4. The study materials and methods

The object of our study is the stressed state of metal under multiparameter influences on roll grip and rolling stability.

The study hypothesis assumed that by solving a closed problem in plasticity theory using the argument-function method of a complex variable, sophisticated problems could be posed and solved, including loading asymmetry, plastic

deformation effects, extreme processes, as well as plastic deformation intensity.

The study's assumptions are:

– linearization of boundary conditions and a hyperbolic partial differential equation for determining shear stresses.

Methods used in the solution process:

– argument-function method of a complex variable.

Data sources used in the study:

– theoretical and experimental data from other authors, my experimental study assessing additional effects on the plastic deformation site under laboratory rolling mill conditions.

Software used in the study:

– Mathcad 15 software was used to calculate the stressed state.

5. Results of investigating the stressed state of metal under the influence of multiparametric factors

5. 1. Construction of physical and mathematical models of a plane rolling theory problem taking into account multiparameter factors

The influence of deformation asymmetry as a control factor on the parameters of plastic deformation was demonstrated in [1, 3]. An effect was identified that manifests itself in a decrease in the force load with an increase in the deformation effect.

The physical model of the process is based on experimental data from employees at the South Ukrainian School of Rolling Mills, Dnipro (National Metallurgical Academy of Ukraine) [1].

The experimental setup consists of a manufactured model rolling mill 120...150 mm, which in all respects corresponds to rolling mills in industrial production. The following devices were the main equipment elements of the industrial and research mill: a working stand, where plastic deformation occurs in rotating rolls; two spindles, which transmit rotation and load to the working rolls of the mill at an angle from the gear stand. A gear cage designed to split the rotation between the rolls and the load; a gearbox used to reduce the speed and increase the load; coupling clutches and an electric drive. The primary device for implementing plastic deformation was the working cage. Main components: two working rolls, two closed-type frames; four bearing housings (cushions) for the roll necks; rulers, guides, pressure tables, and balancing devices.

A point load cell mounted in the rolls was used to measure contact stresses. The primary loading element of the point load cell is a rod element subject to bending and compression. A half-bridge circuit was developed to connect the sensors to the rod element. An amplifier, oscilloscope, and connecting cables were used. Unique experimental data was obtained.

The following process parameters were used. The rolling technology used to measure contact stresses was a simple case of rolling in rolls of the same diameter, without the use of external longitudinal forces. The strip was fed into the gap between rotating rolls, and the rolls gripped the metal through contact friction. In the deformation site, the strip was reduced in height. The strip was lengthened and increased in width. This technology is used for rolling strips, or strips of medium and wide widths.

The main similarity criteria were represented by relative values: the deformation site shape factor, representing the ratio of the deformation site length to the average thickness; the friction coefficient; and the relative reduction. Parameter variations were assumed to be limiting values, which essentially covered the entire range of their practical application: friction coefficients from 0.05 to 0.50; shape factor from 1.00 to 15.00. These represented the main technological parameters of the rolling process.

The used similarity criteria were sufficient to validate the physical model of the problem set.

The physical model of the process manifests itself in the fact that in the lagging zone, in addition to the compressive longitudinal stresses from contact friction, longitudinal tensile stresses act, manifesting themselves as a concavity in the normal contact stress diagrams. Tensile forces arise due to the opposing action of normal pressure forces (the pushing force) and the pulling force of friction at the entrance to the deformation site, Fig. 1. In this case, a backward tension arises from the lagging zone, reducing the length of the leading zone and reducing the contact pressure in the zone of metal reverse movement. The interaction of opposing forces manifests itself most effectively in the initial stage of the process, changing the shape of the contact stress diagrams.

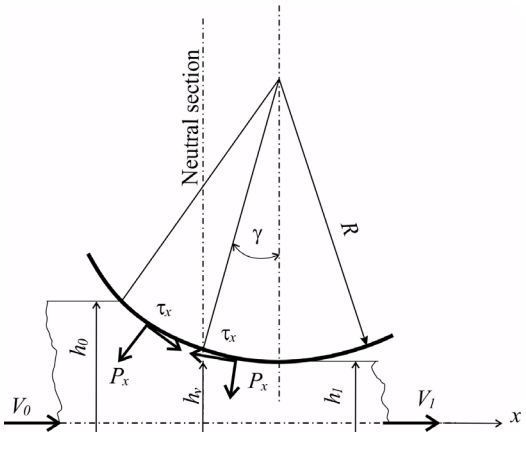

Fig. 1. Diagram of contact forces acting at the deformation site

Thus, the deformation site is subject to vertical compression forces from the normal force and friction, as well as longitudinal tensile forces in the lagging zone. Taking into account the longitudinal tensile force, as well as the ratios of normal and retracting forces, collectively determine the stability of the rolling process and the gripping ability of the rolls.

It should be kept in mind that the gripping of metal by the rolls is the process of forming a stressed and strained state of the metal within a confined space, under given process parameters.

The attainability zone of the ultimate deformation site is shown under conditions of the effect manifesting itself through loss of stability or the process of metal slippage in the rolls. Analysis revealed that the gripping of metal by the rolls is the determining factor in the occurrence of this phenomenon. Therefore, it is necessary to study the influence of the multi-component nature of the rolling process on the conditions and parameters for the formation of the gripping ability of the rolls and the possibility of achieving process stability. For a complete understanding of this problem, the entire deformation site, rather than a partial confined space, is considered.

Fundamental and trigonometric substitutions are used. The system of equations for the closed problem is represented in the following form [6]:

$$\frac{\partial\sigma_x}{\partial x}+\frac{\partial\tau_{xy}}{\partial y}=0,\ \frac{\partial\tau_{yx}}{\partial x}+\frac{\partial\sigma_y}{\partial y}=0,$$

$$(\sigma_x-\sigma_y)^2+4\tau_{xy}^2=4k^2,$$

$$\frac{\sigma_x-\sigma_y}{2\cdot\tau_{xy}}=\frac{\xi_x-\xi_y}{\gamma'_{xy}}=F_1, \quad (1)$$

$$\xi_x+\xi_y=0,$$

$$\frac{\partial^2\xi_x}{\partial y^2}+\frac{\partial^2\xi_y}{\partial x^2}=\frac{\partial^2\dot{\gamma}_{xy}}{\partial y\partial x},$$

$$\frac{\partial^2 T}{\partial y^2}+\frac{\partial^2 T}{\partial x^2}=0,$$

where σ_x and σ_y are normal stresses; τ_{xy} is the shear stress; k is the plastic shear resistance (variable); ξ_x, γ_{xy} are the linear and shear strain rates; T is the metal temperature at a given point.

The boundary conditions are specified in terms of stress and strain rate:

$$\tau_n=-\left[\frac{\sigma_x-\sigma_y}{2}\cdot\sin(2\varphi)-\tau_{xy}\cos(2\varphi)\right], \quad (2)$$

$$\dot{\gamma}_n=-2\left[\frac{\xi_x-\xi_y}{2}\cdot\sin(2\varphi)-\dot{\gamma}_{xy}\cos(2\varphi)\right],$$

where γ_n is the shear strain rate characterizing the boundary condition; τ_n is the shear stress characterizing the boundary condition.

Solving the system of equations (1) and boundary conditions (2) yields a general result for stresses and strain rates. The result is that the deformation and force fields contain identical sets of functions, allowing one to obtain a mathematical model of a plastic medium or simply close the problem in terms of stress fields and strain rates.

Under this statement, the solution in stresses is supported by the solution to the deformation problem, which enhances the reliability of the result and satisfies the energy conditions of interaction in the deformation site [6].

The preliminary result [6] is used to obtain a solution to an applied asymmetric problem in plasticity theory with a limited force component of the process. In this case, the statement is simplified, and the problem is closed by the force characteristics of the process.

Taking into account (1) and (2), a simplified statement of the problem in stresses is obtained and used:

– differential equilibrium equations

$$\frac{\partial\sigma_x}{\partial x}+\frac{\partial\tau_{xy}}{\partial y}=0,\ \frac{\partial\tau_{yx}}{\partial x}+\frac{\partial\sigma_y}{\partial y}=0; \quad (3)$$

– Huber-Mises equation of plasticity

$$(\sigma_x-\sigma_y)^2+4\tau_{xy}^2=4k^2; \quad (4)$$

– differential equation of continuity of deformation in stresses

$$\Delta^2 n\sigma_0=\frac{\partial^2 n\sigma_0}{\partial x^2}+\frac{\partial^2 n\sigma_0}{\partial y^2}=0; \quad (5)$$

– boundary conditions

$$\tau_n=-\left[\frac{\sigma_x-\sigma_y}{2}\cdot\sin(2\varphi)-\tau_{xy}\cos(2\varphi)\right], \quad (6)$$

where σ_0 is the mean normal stress; n is a constant determined by the problem conditions.

The deformation component of the process (the strain continuity equation) entered the force component through the mean normal stress.

Expression (6), for the boundary conditions, relates the stress tensor components to the shear contact stress. This representation of the shear contact stress (6) introduces significant uncertainties into the process of obtaining the result. To linearize the boundary conditions and the solution itself, the following notation of the boundary conditions is adopted

$$\tau_n=-T_i\sin(A\Phi-2\varphi), \quad (7)$$

where T_i is the intensity of the shear stresses; $A\Phi$ is the unknown function of the coordinates or the first argument of the function; φ is the angle of inclination of the platform. Comparing formulas (6) and (7), it can be shown that the shear stresses for the boundary conditions (6) τ_{xy} and the differences $(\sigma_x-\sigma_y)$ for normal stresses are related via the following expressions

$$\frac{\tau_{xy}}{T_i}=\sin A\Phi,\ \sigma_x-\sigma_y=2\sqrt{T_i^2-\tau_{xy}^2}. \quad (8)$$

In work [23], the well-known differential equation for determining the shear stresses is expressed in terms of the intensity of the shear stresses T_i

$$\frac{\partial^2\tau_{xy}}{\partial x^2}-\frac{\partial^2\tau_{xy}}{\partial y^2}=\pm 2\frac{\partial^2}{\partial x\partial y}T_i\cdot\sqrt{1-\left(\frac{\tau_{xy}}{T_i}\right)^2}. \quad (9)$$

From (8), (9), the transformations determined from expression (7) become clear. A trigonometric substitution of the ratio under the radical was performed, which made it possible to linearize the right-hand side of expression (9) and linearize the boundary conditions. This approach is interesting in that for linear partial differential equations, a fundamental substitution is allowed, accompanied by certain peculiarities. These peculiarities consist in the fact that the exponent is an unknown function. Hence, we obtain

$$T_i=H_\sigma\exp\theta, \quad (10)$$

where θ is an unknown function, or the second argument function. Taking into account the substitutions in expressions (8), (10), we have

$$\tau_{xy}=H_\sigma\cdot\exp\theta\cdot\sin A\Phi. \quad (11)$$

Taking into account transitions (8) to (11), the problem statement is clarified: what mathematical relations must the argument of function (8), (10) satisfy in order to close the solution to the problem, turning hyperbolic equation (9) into an identity. Of interest are generalized fundamental approaches to solving problems in plasticity theory using a function of a complex variable. By substituting expressions (8) and (10) into (11), an expression for the shear stress is obtained through a function of a complex variable

$$\tau_{xy}=H_\sigma\cdot\frac{\exp(\theta+i\cdot A\Phi)-\exp(\theta-i\cdot A\Phi)}{2i}. \quad (12)$$

Using relation (12) and equation (9), the differential equation is expressed in terms of a complex variable:

$$\frac{1}{2i}\exp\left(\theta+i\cdot A\Phi\right)\times$$
$$\times\left\{\begin{array}{l}\left[\left(H_\sigma\right)_{xx}-\left(H_\sigma\right)_{yy}-2i\left(H_\sigma\right)_{xy}\right]+\\+2\left(H_\sigma\right)_x\left[\left(\theta_x+A\Phi_y\right)-i\left(\theta_y-A\Phi_x\right)\right]-\\-2\left(H_\sigma\right)_y\left[i\left(\theta_x+A\Phi_y\right)-\left(\theta_y-A\Phi_x\right)\right]+\\+H_\sigma\left[\left(\begin{array}{l}\theta_{xx}-\theta_{yy}+\\+2A\Phi_{xy}\end{array}\right)+i\left(\begin{array}{l}A\Phi_{xx}-A\Phi_{yy}-\\-2\theta_{xy}\end{array}\right)\right]+\\+H_\sigma\left[\left(\theta_x+A\Phi_y\right)-i\left(\theta_y-A\Phi_x\right)\right]^2\end{array}\right\}-$$
$$-\frac{1}{2i}\exp\left(\theta-i\cdot A\Phi\right)\times$$
$$\times\left\{\begin{array}{l}\left[\left(H_\sigma\right)_{xx}-\left(H_\sigma\right)_{yy}+2i\left(H_\sigma\right)_{xy}\right]+\\+2\left(H_\sigma\right)_x\left[\left(\theta_x+A\Phi_y\right)+i\left(\theta_y-A\Phi_x\right)\right]-\\-2\left(H_\sigma\right)_y\left[\left(\theta_y-A\Phi_x\right)-i\left(\theta_x+A\Phi_y\right)\right]+\\+H_\sigma\left[\left(\begin{array}{l}\theta_{xx}-\theta_{yy}+\\+2A\Phi_{xy}\end{array}\right)-i\left(\begin{array}{l}A\Phi_{xx}-A\Phi_{yy}-\\-2\theta_{xy}\end{array}\right)\right]+\\+H_\sigma\left[\left(\theta_x+A\Phi_y\right)+i\left(\theta_y-A\Phi_x\right)\right]^2\end{array}\right\}=0. \quad (13)$$

Equation (13) has a number of peculiarities. During the transformations, identical brackets $(\theta_x + A\Phi_y)$ and $(\theta_y - A\Phi_x)$ appeared for different operators, and the conditions for the existence of variable H_σ were determined for this equation. For the purpose of simplification, we can move on to the Cauchy-Riemann relations and the Laplace equations. Taking the above brackets equal to zero, we obtain:

$$\theta_x=-A\Phi_x;$$
$$\theta_y=A\Phi_x;\ \theta_{xx}+\theta_{yy}=0,$$
$$A\Phi_{xx}+A\Phi_{yy}=0. \quad (14)$$

The next feature of equation (13) is variable H_σ, which can be represented as

$$H_\sigma=\frac{C_0\cdot\left(\frac{l}{2}-x\right)+C_1\cdot\left(\frac{l}{2}+x\right)}{l}, \quad (15)$$

where C_0, C_1 are constants defining the stresses at the entrance and exit of the deformation site; l is the length of the deformation site.

Variable (15) identifies the asymmetry process along the deformation site, allowing for different boundary conditions to be specified at the entrance and exit of the deformation site.

To solve this problem, it is necessary to develop a theory and mathematical model of the process that take into account the influence of multicomponent factors on the gripping ability of the rolls.

Substituting the Cauchy-Riemann relation (14) into differential equation (13) confirms that it becomes an identity. This allows for the determination of the shear stress value.

Basic expression (11) and the conditions for the existence of solution (14) define the shear stress function as

$$\tau_{xy}=H_\sigma\cdot\exp\theta\cdot\sin A\Phi,$$

at

$$\theta_x=-A\Phi_x;$$
$$\theta_y=A\Phi_x;$$
$$\theta_{xx}+\theta_{yy}=0;$$
$$A\Phi_{xx}+A\Phi_{yy}=0. \quad (16)$$

Another feature of the solution should be emphasized. In equation (13), the derivatives of variable H_σ with respect to the coordinates were determined by dependence on the Cauchy-Riemann relations. This allowed them to be eliminated from further consideration and simplified the problem.

From the equilibrium equations (1), given the known functional dependence (16), the normal components of the stress tensor can be determined. After separating the variables of the equilibrium equations, the following expressions are obtained:

$$\frac{\partial\left(\sigma_x-\sigma_0\right)}{\partial x}=-\left[\begin{array}{l}\left(H_\sigma\right)_y\cdot\exp\theta\cdot\sin A\Phi+\\+H_\sigma\cdot\theta_y\cdot\exp\theta\cdot\sin A\Phi+\\+H_\sigma\cdot A\Phi_y\cdot\exp\theta\cdot\cos A\Phi\end{array}\right];$$
$$\frac{\partial\left(\sigma_y-\sigma_0\right)}{\partial y}=-\left[\begin{array}{l}\left(H_\sigma\right)_x\cdot\exp\theta\cdot\sin A\Phi+\\+H_\sigma\cdot\theta_x\cdot\exp\theta\cdot\sin A\Phi+\\+H_\sigma\cdot A\Phi_x\cdot\exp\theta\cdot\cos A\Phi\end{array}\right].$$

By integrating the equation of continuity of deformations (5), we obtain [1]:

$$\sigma_x=H_\sigma\cdot\exp\theta\cdot\cos A\Phi+\sigma_0+f\left(y\right);$$
$$\sigma_y=-H_\sigma\cdot\exp\theta\cdot\cos A\Phi+\sigma_0+f\left(x\right);$$
$$\tau_{xy}=H_\sigma\cdot\exp\theta\cdot\sin A\Phi;$$
$$\sigma_0=\mp n\cdot H_\sigma\cdot\exp\theta\cdot\cos A\Phi,$$

at

$$\theta_x=-A\Phi_x;\ \theta_y=A\Phi_x;$$
$$\theta_{xx}+\theta_{yy}=0;\ A\Phi_{xx}+A\Phi_{yy}=0. \quad (17)$$

Solution (17) satisfies the equilibrium equations, differential equation (9) or (13), and the deformation continuity equation (5). The question arises: to what extent is the Huber-Mises plasticity condition satisfied? Substituting expressions (17) into equation (4), taking into account $f(y) = f(x) = C$, we obtain

$$\left(\sigma_x-\sigma_y\right)^2+4\tau_{xy}^2=\left(2H_\sigma\cdot\exp\theta\cdot\cos A\Phi\right)^2+$$
$$+4\left(H_\sigma\exp\theta\cdot\sin A\Phi\right)^2=4\left(H_\sigma\cdot\exp\theta\right)^2=4T_i^2.$$

In the case of the Huber-Mises plasticity condition, $T_i = k$, the identical satisfaction of the plasticity condition for a plane problem is obtained, (1)

$$\left(\sigma_x-\sigma_y\right)^2+4\tau_{xy}^2=4k^2.$$

Result (17) fully satisfies the system of equations (3) to (5) in analytical form. Thus, based on the solution to a closed-form problem in plasticity theory, a particular solution to problem (17) is represented in closed form.

When constructing a mathematical model for stressed state analysis under conditions of multi-component influences on the gripping ability of the rolls and the stability of the rolling process, defining boundary conditions were used.

The need to study the influence of multi-component rolling is associated with an additional study of the effect of plastic deformation under conditions of decreasing force impact by increasing deformation loading.

Process limitations are presented, determining a single-zone deformation site with stable process implementation, on the one hand, and the realization of the effect of plastic deformation, on the other.

The main problem is to identify the conditions for the existence of a single-zone deformation site during a stable rolling process.

Using solution (17) and expression (15), the following result is obtained:

$$\sigma_x = -\frac{C_0\cdot\left(\frac{l}{2}-x\right)+C_1\cdot\left(\frac{l}{2}+x\right)}{l}\times$$
$$\times\exp\theta\cdot\cos A\Phi+\sigma_0+f\left(y\right);$$

$$\sigma_y = -\frac{C_0\cdot\left(\frac{l}{2}-x\right)+C_1\cdot\left(\frac{l}{2}+x\right)}{l}\times$$
$$\times\exp\theta\cdot\cos A\Phi+\sigma_0+f\left(x\right);$$

$$\tau_{xy} = \frac{C_0\cdot\left(\frac{l}{2}-x\right)+C_1\cdot\left(\frac{l}{2}+x\right)}{l}\cdot\exp\theta\cdot\sin A\Phi;$$

$$\sigma_0 = -2\frac{C_0\cdot\left(\frac{l}{2}-x\right)+C_1\cdot\left(\frac{l}{2}+x\right)}{l}\cdot\exp\theta\cdot\cos A\Phi, \qquad (18)$$

at $\theta_x = -A\Phi_x$; $\theta_y = A\Phi_x$; $\theta_{xx}+\theta_{yy}=0$; $A\Phi_{xx}+A\Phi_{yy}=0$.

To determine the integration constants, boundary and apparent conditions in the deformation site were used. The origin is placed at the center of the deformation site, and the x-axis is shown in the rolling direction.

At:

$$x=-\frac{l}{2},\ y=\frac{h_0}{2},\ A\Phi=A\Phi_0,\ \theta=\theta_0,$$
$$\sigma_x-\sigma_y=\xi_0 2k_0,\ \tau_{xy}=\psi_0 k_0; \qquad (19)$$
$$x=\frac{l}{2},\ y=\frac{h_1}{2},\ A\Phi=A\Phi_1,\ \theta=\theta_1,$$
$$\sigma_x-\sigma_y=\xi_1 2k_1,\ \tau_{xy}=\psi_1 k_1,$$

where $A\Phi_0$ and $A\Phi_1$, θ_0 and θ_1, k_0 and k_1, ξ_0 and ξ_1 are the values of functions $A\Phi$ and θ at the edges of the deformation site; shear resistance; coefficients taking into account the effects of back pressure and rolling tension at the entrance and exit of the deformation site.

Substituting the boundary conditions (19) into (18), the following result is obtained

$$C_0=\frac{k_0\xi_0}{\exp\theta_0\cos A\Phi_0};\ C_1=\frac{k_1\xi_1}{\exp\theta_1\cos A\Phi_1};$$

$$\psi_0=\tan A\Phi_0;\ \psi_1=\tan A\Phi_1. \qquad (20)$$

Comparing expressions (18) to (20), we conclude that the obtained data allow us to consider asymmetry along the deformation site length and take into account changes in the stressed state.

To further analyze the stressed state under asymmetric loading (18), it is necessary to determine the argument of function θ and $A\Phi$. The mathematical model provides this capability. By solving Laplace's equations and matching the result with the Cauchy-Riemann conditions, the first argument function for the trigonometric dependence is obtained

$$A\Phi' = AA_6'\cdot\left(\frac{l}{2}+x\right)\cdot y - AA_6''\cdot\left(\frac{l}{2}-x\right)\cdot y-2\varphi=$$
$$=AA_6'\cdot\left[\left(x-X_0\right)+\left(\frac{l}{2}+X_0\right)\right]\cdot y+$$
$$+\ AA_6'\cdot\left[\left(x-X_0\right)-\left(\frac{l}{2}-X_0\right)\right]\cdot y-2\varphi, \qquad (21)$$

where $\varphi=(l/2-x)/R$ is the angle of inclination of the contact area; x_0 is the position of the neutral cross-section relative to the origin; AA_6' and AA_6'' are constants defining the values of trigonometric functions at the edges of the deformation site, taking into account the influence of the process kinematics on the force characteristics of the deformation site.

Let us consider and comment on the use of boundary conditions that determine the reliability of the qualitative and quantitative indicators of the problem being solved. Let us dwell on this in more detail.

The coordinates of the point at the exit from the deformation site are $x=l/2$, $y=h_1/2$. The angle of inclination of the area at the exit from the deformation site is $\varphi=0$. The kinematic component in the complex of parameters at the exit from the deformation site is $A\Phi'=(A\Phi_1-\alpha)$. The friction index and the angle of capture are $A\Phi_1$, and α. The coordinates of the point at the entrance to the deformation site are $x=-l/2$, $y=h_0/2$. The angle of inclination of the platform at the entrance to the deformation site is $\varphi=\alpha$. The kinematic component in the complex of parameters at the entrance to the deformation site is $A\Phi'=-A\Phi_0$.

Substituting the boundary conditions into expression (21), we obtain

$$AA_6'=2\frac{A\Phi_1-\alpha}{l\cdot h_1};\ AA_6''=2\frac{A\Phi_0+2\alpha}{l\cdot h_0}. \qquad (22)$$

The integration constants (22) influence the nature of stress distribution at the deformation site and the kinematic rolling conditions, which are designated to a certain extent by the neutral angle. This thereby adds a multi-component approach to the process for assessing the stressed state, including the asymmetry of the distribution along the deformation site.

As analysis reveals, expressions (22) to some extent characterize the interaction of the lag and lead zones. Taking into account the Cauchy-Riemann relations and the Laplace equations (17), function θ is determined

$$\theta=-\frac{1}{2}\cdot\left(AA_6'+AA_6''\right)\cdot\left[\left(x+X_0\right)^2-y^2\right]-$$
$$-\left(AA_6'\cdot l_{om}-AA_6''\cdot l_{on}\right)\cdot\left(x-X_0\right). \qquad (23)$$

Taking into account (21) and the boundary conditions, the neutral angle is determined, showing the position of the neutral section at the deformation site

$$\gamma = \frac{\alpha}{2}\frac{A\Phi_1 - \alpha}{\left(A\Phi_0 + 2\alpha\right)\left(1 - \frac{1}{2}\varepsilon\right)}, \quad (24)$$

where $(A\Phi - \alpha)$ is the kinematic component; ε is the relative compression.

In the kinematic component (24), the friction index, taking into account the obvious conditions of the deformation site, can be represented as

$$A\Phi_1 = A\Phi_0 = f\left(a - b\cdot f\right), \quad (25)$$

where a and b are constants characterizing the friction coefficient at the entrance and exit of the deformation site, and f is the friction coefficient.

When solving kinematic problems, it becomes necessary to address the kinematics of the process when the advance zone is zero. In this case, the relationship between the friction coefficient and the grip angle is reduced to the following form

$$f\left(a - b\cdot f\right) - \alpha = bf^2 - af + \alpha = 0.$$

An expression for obtaining the coefficient of friction has been determined

$$f = \frac{a \pm \sqrt{a^2 - 4b\alpha}}{2b}. \quad (26)$$

At $a = b = 1$, we have

$$f = \frac{1 \pm \sqrt{1 - 4\alpha}}{2}. \quad (27)$$

Using expression (23), taking into account the boundary conditions, we determine the integration constants θ_1 and θ_2:

$$\theta_1 = -\frac{1}{2}\cdot\left(AA'_6 + AA''_6\right)\cdot\left(l_{om}^2 - \frac{h_0^2}{4}\right) + \\ + \left(AA'_6\cdot l_{om} - AA''_6\cdot l_{on}\right)\cdot l_{om},$$

$$\theta_2 = -\frac{1}{2}\cdot\left(AA'_6 + AA''_6\right)\cdot\left(l_{on}^2 - \frac{h_1^2}{4}\right) + \\ + \left(AA'_6\cdot l_{om} - AA''_6\cdot l_{on}\right)\cdot l_{on}.$$

Using expressions for C_σ taking into account dependences (20), working formulas were derived for calculating the stressed state of the strip during rolling, including for a single-zone deformation site (with limited gripping capacity of the rolls):

$$\sigma_x = -\frac{\frac{k_0}{\cos A\Phi_0}\left(\frac{l}{2} - x\right)\exp\left(\theta - \theta_0\right) + \frac{k_1}{\cos A\Phi_1}\left(\frac{l}{2} + x\right)\exp\left(\theta - \theta_1\right)}{l}\cdot\cos A\Phi + k_0;$$

$$\sigma_y = -3\frac{\frac{k_0}{\cos A\Phi_0}\left(\frac{l}{2} - x\right)\exp\left(\theta - \theta_0\right) + \frac{k_1}{\cos A\Phi_1}\left(\frac{l}{2} + x\right)\exp\left(\theta - \theta_1\right)}{l}\cdot\cos A\Phi + k_0; \quad (28)$$

$$\tau_{xy} = \frac{\frac{k_0}{\cos A\Phi_0}\left(\frac{l}{2} - x\right)\exp\left(\theta - \theta_0\right) + \frac{k_1}{\cos A\Phi_1}\left(\frac{l}{2} + x\right)\exp\left(\theta - \theta_1\right)}{l}\cdot\sin A\Phi.$$

The values of relative contact specific pressures were calculated using formulas (28). Fig. 2 shows the stress distribution along the length of the deformation site as a function of shape factor l / h [1], which awaits its physical and theoretical justification.

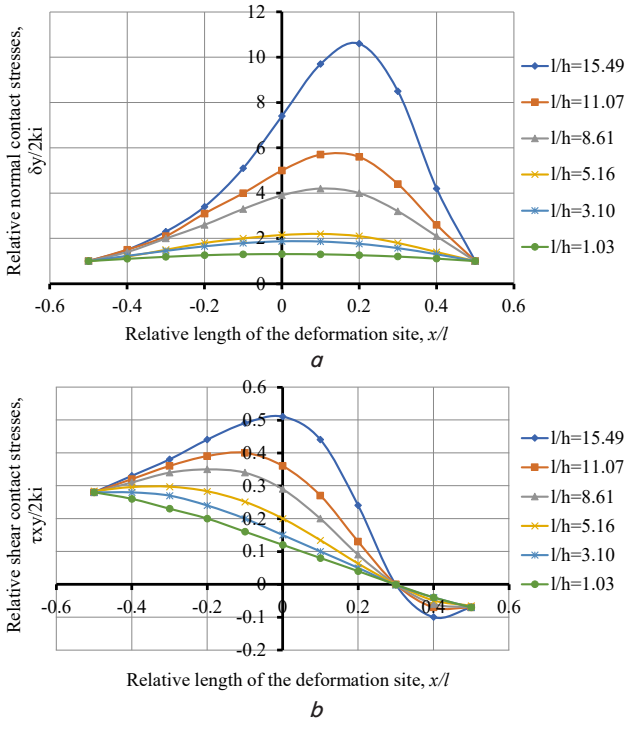

Fig. 2. Distribution of contact stresses along the length of the deformation site depending on the shape factor at $l / h = 1.03...15.49$; $\alpha = 0.077$; $f = 0.3$: *a* – distribution of normal stresses; *b* – distribution of shear stresses

This pattern of contact stress distribution is further confirmed by the experimental diagrams in chapter 5. 3.

Changes in the stressed state in the processing zone are noted depending on the specified factor. Concave and convex contact stress diagrams are observed in different areas of the deformation site. All of this confirms the response of the mathematical model to the adopted physical interpretation of the process. The position of the maximum normal stresses along the deformation site, as well as the magnitude of the contact stresses, changes. In terms of shear stresses, the stability of the rolling process is confirmed by the presence of a leading zone.

Based on the data analysis, a key feature of this approach is the equivalence of the effects of the shape factor and the tension from the lagging zone, which determine the kinematics of the process and the force characteristics of the reduction zone. Given this formulation of the question, this assertion must be substantiated and proven.

This proof must be provided by identifying process features through the gripping ability of the rolls and the stability of the rolling process. This approach is crucial for further research.

5. 2. Results of investigating the process of minimum stability, the process of partial suppression of zeroing factors of the stressed state

Based on work [1], which confirms similar approaches to plastic deformation effects, the possibilities of determining the process mechanism through the multicomponent factor and the characteristics of the roll gripping ability were considered. The processes of metal gripping by rolls and the conditions for implementing a stable rolling process are investigated depending on a number of determining factors: contact friction, through the friction coefficient; reduction; and the shape factor. Obviously, these factors will also influence not only the gripping ability of the rolls but also the achievability of the limiting deformation site effect.

Existing advancements on metal gripping by rolls [10] prove insufficient to explain many theoretical and practical aspects of the process, necessitating a revision of the conditions for implementing the roll gripping ability and the conditions for loss of process stability. These include:

– concavity of the normal stress diagrams in the lag zone and along the entire length of the deformation site;

– absence of plastic deformation during roll slippage, explanation of the mechanics of negative lead [24];

– absence of a lead zone during roll gripping;

– phenomenon of contraction of the height of the rolled product before entering the deformation site [12].

The answers to these questions are closely related to the adopted physical model of the rolling process: accounting for the influence of tensile stresses in the lagging zone on the force and deformation characteristics of the rolling process. In this regard, these issues are examined in greater detail. It is known that the initial grip of the metal by the rolls occurs under conditions where the pulling forces of contact friction are no less than the normal pushing forces from the rolls. Moreover, the grip of the metal by the rolls during a steady-state process can be greater than the initial angle by up to two values of the initial grip. It follows that, having overcome the grip at the initial moment, it is possible to double the grip angle without losing the stability of the process. In [1], it is proposed, based on the solution to a plane problem of plasticity theory, to characterize the gripping capacity not only by contact diagrams of tangential stresses but also by normal stresses. Following [1], it is shown that the loss of stability is determined not by one but by two factors – grip and the degree of stretching of the lagging zone in the processing area, Fig. 1, determined by the physical model of the process. When assessing the influence of these two parameters on the stability of the process, it is necessary to focus on the tangential and normal stresses that react to the stretching of the strip in the lagging zone.

Shear stresses vary along the deformation site, crossing the zero line in the neutral section. If there is no zero crossing, there is no lead zone, and a loss of stability, i.e., slippage, should occur. Normal stresses provide another criterion for assessing the stability of the rolling process: rolling under rear strip tension from the lagging zone, which affects stability, the shape of the normal contact stress diagrams, and the magnitude and kinematics of processing. The concavity of the diagram is a qualitative and quantitative assessment of the tensile effect in the lagging zone or along the entire length of the deformation site. Such approaches are known in the literature; however, strip stretching has not been linked to process stability or the gripping capacity of the rolls. It should be noted that a decrease in contact stresses below permissible limits, i.e., a concavity of the relative stress diagram less than unity or stresses less than the yield strength, indicates the absence of plastic deformation. Then the rolling process as such does not exist, there is no gripping, no stability.

This connection between strip stretching, plastic processing, process stability, and the gripping capacity of the rolls is the defining and indicative reason for the emergence of a new process quality, an additional force and kinematic effect on the plastic forming zone.

It follows that processes that contribute to deformation accompany the process of metal gripping by the rolls. The presence of plastic deformation is obviously determined by the multi-component impact on the reduction zone.

There are examples of the influence of factors that ensure the presence of deformation of the rolled product during the moment of metal gripping by the rolls. Studies [12, 24] have shown that at the entrance to the deformation site, there is a contraction of the strip along the height of the rolled product. This indicates the presence of tensile stresses throughout the lagging zone, the thinner the strip, the greater the stress. Thus, in the lagging zone, the strip is contracted along the height, which corresponds to the physical model in [1]. Another example of plastic deformation that enhances metal gripping by the rolls is the impact plastic action of the workpiece on the contact surface of the rolls. Localized contact between the workpiece and the rolls at the entrance to the deformation site results in localized plastic deformation, which ensures metal gripping by the rolls [10]. The next argument in favor of the deformation component during gripping is rolling with a negative lead [23]. These studies demonstrate that stable rolling occurs not only in the absence of a lead zone, but also under process conditions where the peripheral speed of the rolls is greater than the speed of the strip exiting the deformation site. Thus, plastic deformation of the strip is permitted beyond the known limits of the initial grip of the metal by the rolls. In this case, the fact of such a phenomenon is important. Finally, it should be noted that factors contributing to the presence of plastic deformation at the moment of gripping are parameters that enhance the process. This must be taken into account when assessing the impact on the gripping ability of the rolls and the loss of rolling stability.

Based on the proposed physical model of roll gripping ability and the argument-function method for solving problems in continuum mechanics, the theoretical part and mathematical model for the process boundary has been worked out. This allowed us to explore the area where roll slippage partially occurs. In this state, representing the stage of interaction between multidirectional forces within the deformation site, signs of additional influence on the deformation site can be detected. These influences manifest themselves in the zones where the ultimate deformation site is reachable, within the parameters of the process.

It is possible to clearly evaluate the stressed state of the strip when the rolls grip beyond their ultimate limit. It should be noted that slippage of the rolls is a loss of rolling stability. Ultimate roll grip is defined as gripping at the point of process instability; beyond-ultimate roll grip is defined as roll gripping beyond the process boundary. Although beyond-ultimate grip presupposes roll slippage, the working variant is the stress distribution during roll slippage, if the mathematical model of the process allows it.

Fig. 3 shows diagrams of the beyond-limit metal gripping capacity of the rolls for different form factor values and a friction coefficient of 0.015, which is less than the grip angle of 0.077. Their ratio is significantly less than unity, equal to 0.195.

If this ratio equals unity, the gripping capacity of the rolls is fixed under stable rolling conditions. Since the process is beyond the limit, there is no metal gripping by the rolls, which is confirmed by the diagrams of shear and normal stresses, Fig. 3.

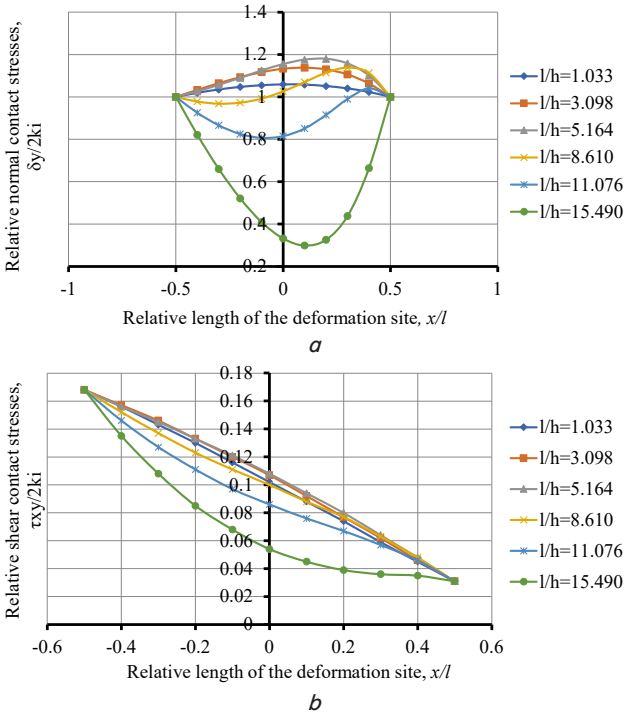

Fig. 3. Distribution of contact stresses along the length of the deformation site under conditions of extreme grip of metal by rolls at $l / h = 1.033...15.49$; $f = 0.015$; $\alpha = 0.077$: *a* – distribution of normal stresses; *b* – distribution of shear stresses

Deflections in the normal and shear stress diagrams are observed, indicating the presence of tensile stresses from the lagging zone. Consequently, the pushing force is greater than the pulling force, i.e., the contact friction force. The relative shear stresses are maximum at the entrance to the deformation site (0.168) and minimum at the exit from the lagging zone (0.031), not reaching the zero line and, therefore, not crossing it. Deflections in the diagrams occur for the same shear stress values as for normal stresses. Moreover, for diagrams of 1.033...5.164, the limits of variation in shear stress deflections remain unchanged, as there are no changes in friction or the conditions under which the metal is gripped by the rolls.

Analysis of the beyond-limit process reveals that the high strips respond weakly to tensile stresses from the lagging zone. When metal is gripped by rolls, the deflections in the diagrams showing the effects of this stretching will be minimal or absent altogether.

The response of tall strips to stretching in the beyond-limit process to some extent reflects the mechanics of the process with negative lead, which allows for the absence of a lead zone when metal is gripped by rolls and the presence of a grip with negative metal flow kinematics [24]. Consequently, there are processes in which stable rolling occurs not only with zero lead, but also in processes in which the peripheral speed of the rolls is higher than the strip velocity at the exit from the deformation site. Thus, at the present stage, the criterion of roll gripping ability, which is currently determined by the ratio between the normal pushing force and the frictional gripping force, is not fully justified. To explain the above features, another factor must be present that nullifies the process in the presence of a tensile force in the lag zone.

The kinematics of the process under conditions of ultimate capture have been considered. The multidirectional action of forces on the deformation site creates a backlash on the deformed strip. This backlash affects not only the force parameters but also the kinematic parameters of the process. Thus, two factors associated with process instability are formed: the grip and the process determined by the action of tensile forces from the lagging zone. Ultimately, a process with concavity or convexity of the normal stress diagrams is formed. The above-described regimes may differ in their interaction conditions, counteract each other, or coincide. The tensile factor determines the process of the ultimate deformation site, which is a fundamental indicator of the plastic deformation effect. It should be noted that the proposed approach does not claim to fundamentally change the theory of roll gripping ability at small grip angles and friction coefficients. However, in the extreme case, it registers the emergence of a new quality, which to a certain extent characterizes the process of plastic deformation under conditions of negative lead or lead tending to zero.

As for the stability of the process, the buckling diagram for shear stresses to a certain extent replicates the buckling diagram for normal stresses. The partial or complete concavity of the normal stress diagrams relative to unity (Fig. 3) is partially or completely replicated by the concavity of the shear stress diagram.

Fig. 4 shows the rolling process with a minimum grip angle of 0.077, but with an increased friction coefficient of 0.085, which ensures primary capture in the absence of a lead zone. This process became possible after introducing a second influencing factor, the effect of tension on the stressed state parameters at the deformation site. A preliminary analysis of shear stresses indicates no capture, while for normal stresses, capture is ensured by the presence of plastic deformation in the lagging zone (there is no deflection of the diagram below the limit line, whose ordinate is equal to unity). The ratio of the friction coefficient to the grip angle, which creates primary capture, is 1.10. Consequently, metal capture by the rolls is ensured in the absence of a lead zone. It follows that the lead zone is not a criterion for roll gripping capacity.

Analysis reveals that with an increase in the shape factor from 1.033 to 5.614, the maximum normal contact stresses increase within the range of 1.132 to 1.602. Subsequently, the stresses increase to 1.998 for a factor of 8.61, and further to 2.586 for a shape factor of 15.49. Concurrently, the load in the lagging zone decreases. For a shape factor of 15.49, up to three curves decrease downwards, including a shape factor of 3.098 (Fig. 4).

This confirms the effect of plastic deformation, i.e., a decrease in the force load with an increase in the deformation component (the deformation component of the process, the shape factor of the deformation site), throughout most of the deformation site.

Compared to the process shown in Fig. 4, the main influencing factors determining the ambiguity of the metal gripping process by the rolls are confirmed and enhanced. On the one hand, the friction coefficient is greater than the grip angle, which characterizes the stability of the process; on the other hand, the absence of a lead zone characterizes the loss of rolling stability. This seemingly contradictory phenomenon can be explained by introducing a lag zone stretching factor, which characterizes the stability of the rolling process. The first three

thicknesses (shape factors 1.033; 3.098; 5.164) (Fig. 3, 4) show that at small grip angles and low friction coefficients, the stretching factor is ineffective. When rolling medium and thin strips, the influence of tensile stress in the lag zone increases, and dips in the contact stress diagrams appear, the larger the dips, the thinner the strip. Maximum stresses respond consistently to an increase in the friction coefficient (1.132; 1.353; 1.602; 1.998; 2.269; 2.586), and stresses in the lagging zone respond consistently to an increase in tensile stresses of opposing forces (abscissa axis – 0.2 at 1.107; 1.261; 1.383; 1.485; 1.474; 1.31). The diagrams of curves, for normal stresses, show the zones of attainability of the limiting deformation site, but do not cross the permissible lines of process stability.

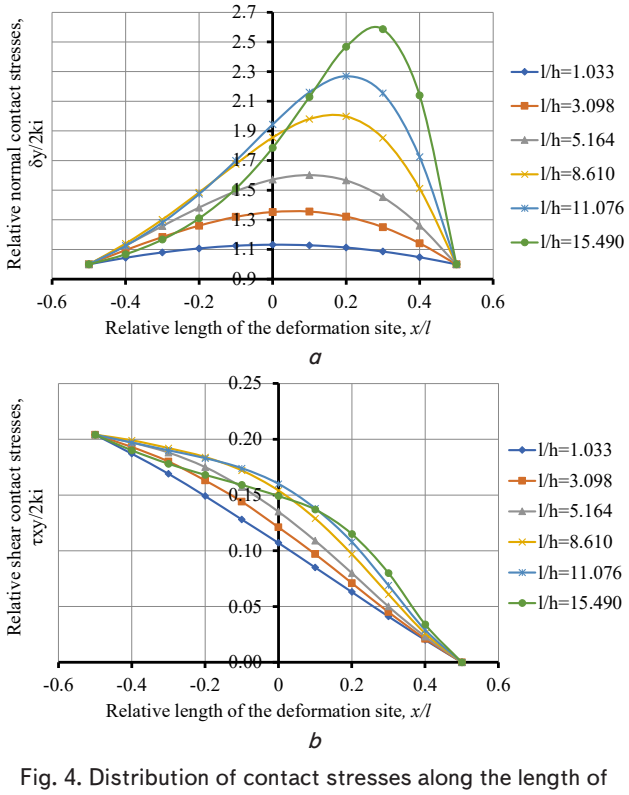

Fig. 4. Distribution of contact stresses along the length of the deformation site when metal is gripped by rolls under transient process conditions, $l/h = 1.033...15.49$; $f = 0.085$; $\alpha = 0.077$: *a* – distribution of normal stresses; *b* – distribution of shear stresses

Of interest is the combination of a zero lead zone and the metal gripping by the rolls (Fig. 4). According to the physical gripping model, with a corresponding ratio of the friction coefficient to the grip angle greater than unity (1.10), metal gripping by the rolls is ensured. A lead zone must also exist. The question arises as to why, with an increase in the friction coefficient, the tensile force increases but not the lead zone, which are mutually opposite. The tensile force arises from the action of two opposing friction forces and normal pressure in the lag zone. A back tension exists at the entrance to the deformation site. As the gripping force increases, the deformation site is restructured, and the lead zone increases. However, when considering the kinematics of metal flow, the back tension at the entrance to the deformation site reduces the lead zone. Moreover, during a steady-state process, based on the law of action and reaction, the oppositely directed normal pressure force increases, increasing the tensile force. With a low friction coefficient and increased tensile force, eliminating the lead zone becomes sufficient. It is hypothesized that with a significant increase in the friction coefficient, the gripping ability of the friction force increases and becomes sufficient to neutralize the tensile force.

The peculiarity of this analysis is that such a process can exist in principle. Due to the increased tensile load in the lagging zone, with an increasing gripping friction coefficient, conditions arise for gripping in the absence of a leading zone. Indeed, the trailing tension alters the kinematics of the deformation site, reducing the leading zone (roll exit). Thus, introducing the tensile force into the analysis makes it possible to evaluate the additional impact by adjusting the gripping process under tensile stresses. Consequently, the process under consideration, with a zero leading zone, can be characterized as transient as it contains elements of a process with loss of stability and elements of a stable rolling process. Clearly, the concept of a transient rolling process should be expanded, linking it to the effect of a limiting deformation site.

The next feature is the realization, within this process, of a zone where the ultimate deformation site can be reached. This is clearly confirmed by the curve diagrams in Fig. 5, even at the minimum grip angle. This transient process serves as a benchmark for designing a rolling force system using the plastic deformation effect. Ultimately, a transient process with minimal stability, or a regime on the verge of process stability, is demonstrated.

Fig. 5 shows the distribution of contact stresses depending on the form factor with a minimum grip angle of 0.077 radians, with the presence of a full-fledged lead zone determined by a friction coefficient of $f = 0.15$.

This is significantly higher than the previous friction values shown in Fig. 4. The ratio of the friction coefficient to the grip angle in this case is 1.95. This is twice the ratio specified for the transient process. There are no signs of loss of stability, either in terms of tangential or normal stresses. The need for such consideration stems from the comparison of a process in which, due to the increasing friction coefficient, the influence of the reachable zone of the ultimate deformation site is minimal. The manifestation of the reachable zones is clearly demonstrated by comparing Fig. 4, 5.

With an increase in the form factor, a steady increase in the maximum contact stresses along the processing zone was observed: 1.195; 1.534; 1.940; 2.707; 3.334; 4.637. In the lagging zone, no decrease in the diagrams below the previous form factor numbers was observed, as was present for the transition deformation site. However, there is a superposition of concavity of the diagrams in the lagging zone at different sections of the deformation site length. For shear stresses, a stable convexity of the shear stress diagrams appeared along the length of the processing zone. The change in shear stresses is within the range of 0.025...0.233, which indicates the lead zone.

To evaluate the convexity of the diagrams, within the zero abscissa of the relative values of shear stresses, we have 0.111; 0.133; 0.157; 0.198; 0.222; 0.246. As can be seen, the convexity of the shear stress diagrams increases with increasing shape factor.

In the lead zone, the shear stress diagrams are concave, due to a change in sign. The lead zone is defined by increased roll gripping ability in terms of shear stresses. For this rolling process, tensile stress factors, i.e., the zone where the limiting deformation site is attainable, are virtually absent. Tensile stresses are suppressed over almost the entire length of the deformation site. Unlike the process in Fig. 4, a new feature has emerged, where the increased tensile force from the increasing friction coefficient is suppressed by the increasing

roll gripping ability (Fig. 5). The exception is the last curve, corresponding to shape factor 15.49, for the thinnest-walled strip. Indeed, analysis of the result reveals a slight decrease in specific pressures in the lag zone for this curve. Table 1 give contact stress data in the lag zone for shape factor 15.49.

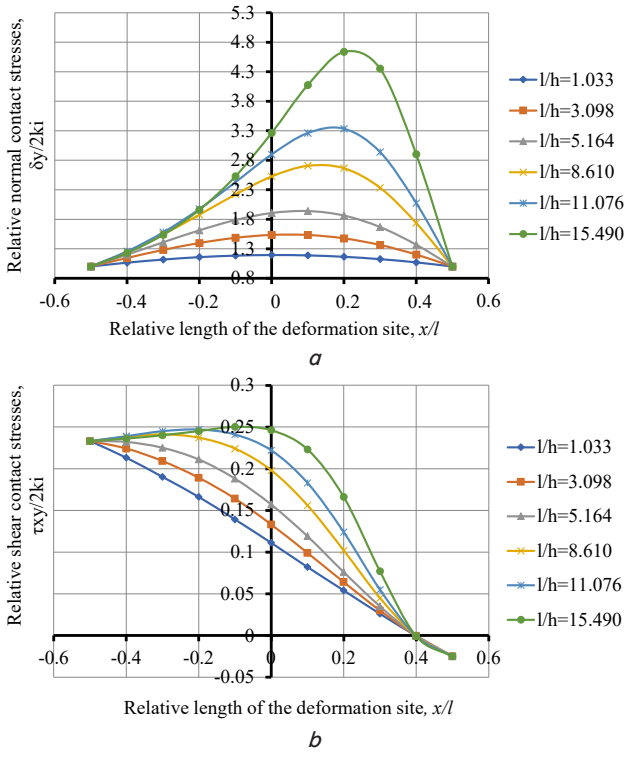

Fig. 5. Distribution of contact stresses along the deformation site during metal gripping by rolls under the conditions of the determining process $l / h = 1.033...15.49$; $f = 0.15$; $\alpha = 0.077$: *a* – distribution of normal stresses; *b* – distribution of shear stresses

Table 1

Comparative data on relative normal contact stresses in the lag zone of the determining process $\alpha = 0.077$ rad

Relative length in the lagging zone, x / l	Deformation site shape factor, l / h					
	1.033	3.098	5.164	8.61	11.07	15.49
	Relative normal contact stresses, $\sigma_y / 2k_i$					
–0.1	1.185	1.485	1.788	2.221	2.429	2.529
–0.2	1.159	1.397	1.613	1.877	1,972	1.959
–0.3	1.118	1.280	1.410	1.544	1.578	1.537
–0.4	1.065	1.144	1.201	1.250	1.256	1.229
–0.5	1	1	1	1	1	1

At the beginning of the lagging zone, the well-known stress-shape factor dependence is still evident, with the abscissa at –0.1. As the shape factor increases, contact stresses increase within the range of 1.185 to 2.529. At abscissas of –0.2 to –0.5, for a factor of 15.49, a slight decrease in normal stresses is observed at the end of the lagging zone. Although this is an insignificant fragment compared to the overall sample, the decrease can be explained by the small, but significant, influence of tensile stress in the lagging zone for thin strips.

A distinctive feature of this process, with a minimum grip angle of 0.077 radians and a two-factor roll gripping capacity, is the suppressive effect on tensile stresses in the lagging zone.

Fig. 6 shows diagrams of the beyond-limit process of metal gripping by rolls for different shape factor values, a minimum friction coefficient of 0.05, and an increased grip angle of 0.129. The ratio of the friction coefficient to the grip angle is less than unity, equal to 0.388. With increasing curve concavity, this is almost twice as large as the analogous ratio for Fig. 3. However, the process is also beyond the critical point.

Note the number of curves analyzed. The curve for shape factor 15.49 is not shown here. Even in Fig. 3, the curve's concavity indicated that its process capabilities were below the critical point. At high friction coefficients, this process occurred at the largest zones of attainable limit deformation, i.e., the load decreased relative to the lower deformation load.

The shear and normal stress diagrams confirm the beyond-critical metal gripping by the rolls (Fig. 6), with the difference that instead of a grip angle of 0.077 radians, a grip angle of 0.129 radians is used, which changes the process parameters.

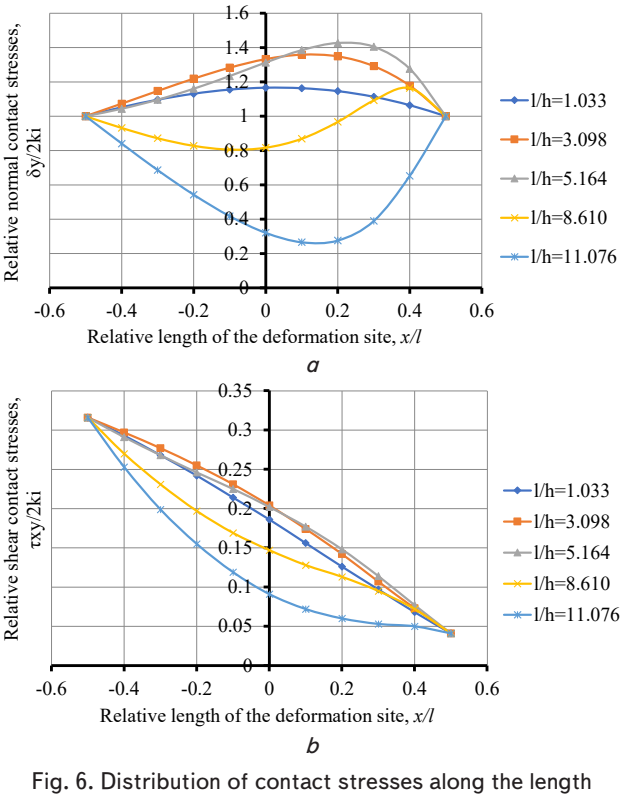

Fig. 6. Distribution of contact stresses along the length of the deformation site under conditions of extreme grip of metal by rolls at $l / h = 1.033...11.07$; $f = 0.05$; $\alpha = 0.129$: *a* – distribution of normal stresses; *b* – distribution of shear stresses

The relative shear stresses, in comparison with the grip angle of 0.077 radians (0.168...0.031) have increased and have a maximum value at the entrance to the deformation site (0.316) and a minimum at the exit from the lag zone (0.041), without reaching the zero line, therefore, without crossing it. There is no lead zone. From this it is evident that there has been an increase in shear stresses as a response to the increase in the grip angle. Normal stresses also respond to the increase in the grip angle. Whereas the processes in Fig. 3 show a decrease in the process load on curves 8.61 (partial loss); 11.07; 15.49, in Fig. 6 the deflections of the normal stress diagrams occur with the shape factors 8.61; 11.07; 15.49 (thin stripes). Curve 5.164 has moved downwards, under the previous number 3.098 in the

lag zone, Fig. 6. Moreover, curve 15.49 fell within the attainability zone already in the processes shown in Fig. 4. There is no loss of stability in the process for only two diagrams (1.033; 3.098), instead of three (Fig. 3). Deflections occur for the same curves in the shear stress diagrams.

Analysis of the stress diagrams between the abscissas of –0.2 and 0.2 was performed; the distribution patterns of these diagrams are different (Fig. 6). Table 2 gives comparative data on the contact stresses at the entry and exit of the deformation site. On the exit side, these are the abscissas with a positive sign, while on the entry side, the abscissas are the minus sign. According to Fig. 2, the larger the shape factor, the greater the normal stresses should be.

Table 2

Comparative data on relative normal contact stresses from the side of the entrance and exit from the deformation site of the beyond-limit process, $\alpha = 0.129$ rad

Deformation site shape factor, l / h	Relative length of the deformation site, x / l				
	0.2	0.1	0.0	–0.1	–0.2
	Relative normal contact stresses, $\sigma_y / 2k_i$				
3.098	1.349	1.359	1.333	1.283	1.219
5.164	1.427	1.385	1.313	1.234	1.160

Indeed, at a shape factor of 5.164, normal stresses increase along the deformation site toward the exit. An increase in stress is also observed toward the exit for a shape factor of 3.098 up to and including the abscissa of 0.1. When comparing curves 5.164 and 3.098 over the range of 0.2 to 0.1, as expected, the values with the shape factor in ascending order correspond to the larger values. However, in the lag zone, the stressed state has reversed, starting from the abscissa of 0.0. Stresses with a shape factor of 3.098 in the lag zone correspond to larger values. Thus, the curve at the ultimate capture, number 5.164, is the fourth stressed state curve that responded to an increase in the grip angle by reducing the load in the lag zone.

A characteristic feature of this process is the increase in tensile force due to the increase in the grip angle and its effect on the ultimate capture of the metal by the rolls. As the grip angle increases, the effect on the normal force in the direction of entry into the deformation site increases. According to the law of action and reaction, the frictional force also increases, which is indicated by an increase in shear stress values. The tensile force and stress, or the rear tension force from the lagging zone, also increases. It should be noted that in the previous processes, the tensile force also increased, but due to an increase in the friction coefficient, not the grip angle. The increased rear tension reduces the capture capacity of the rolls. In the extreme state, the process conditions deteriorate even more, as evidenced by the increased number of curves with concave contact stress shapes, Fig. 6.

Fig. 7 shows the contact stress curves for the transitional deformation site, with a grip angle of 0.129; shape factors of 1.033...11.07.

The rolling process is shown with a grip angle of 0.129, but with a friction coefficient sufficient to achieve primary metal gripping by 0.153 rolls, in the absence of a lead zone. The ratio of the friction coefficient to the grip angle is 1.19, which is greater than for a grip angle of 0.077 radians. A similar pattern of process existence with a zero lead zone is evident, as with a grip angle of 0.077 radians. A transient process also occurs for a grip angle of 0.129 radians, with a slight increase in the ratio of the friction coefficient to the grip angle. The increase in the ratio was 0.09. The capabilities of the physical and mathematical model made it possible to determine the friction coefficient for which the lead zone is absent, and the feasibility of implementing the process at an angle of 0.129 radians in a stable rolling mode.

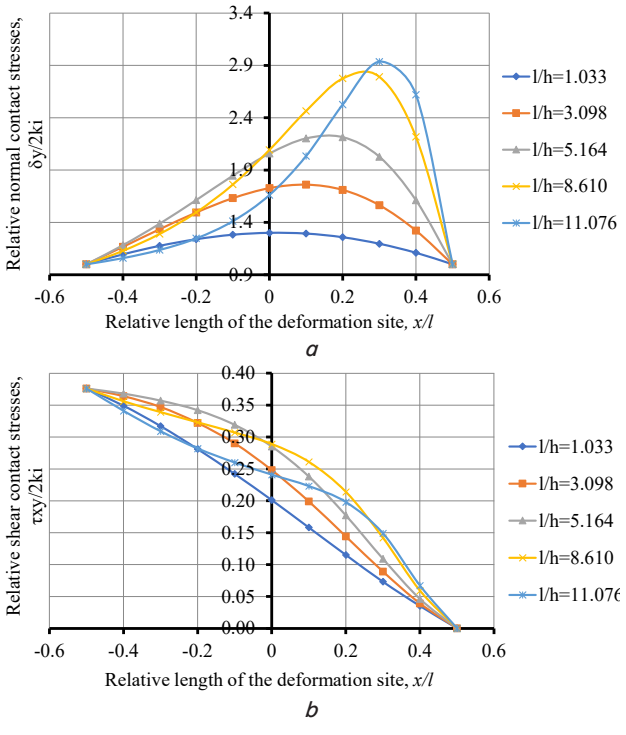

Fig. 7. Distribution of contact stresses along the length of the deformation site when metal is gripped by rolls under transient process conditions at $l / h = 1.033...11.07$; $f = 0.153$; $\alpha = 0.129$: *a* – distribution of normal stresses; *b* – distribution of shear stresses

The trends identified in the ultimate deformation site (Fig. 6) are confirmed in the transient process, Fig. 7.

An analysis of the characteristics of the transient process with changes in the source loading was performed. With an increase in the grip angle, there was an increase in the maximum normal contact stresses for all form factors compared to the transient process, Fig. 4. An increase in the form factor contributed to an increase in the maximum contact stresses, respectively 1.293; 1.761; 2.215; 2.791; 2.936. At the same time, for the same diagrams in the lag zone with an abscissa of –0.2, the following distribution was obtained: 1.239; 1.495; 1.614; 1.496; 1.247. There was a decrease in the contact stresses in the lag zone for higher form factor values. According to Fig. 7, the curve for diagram (8.61) moved lower by two positions, curve (11.07) moved lower by three positions, Fig. 7, which confirms the effect of plastic deformation. These movements of the curves indicate the presence of zones of attainability of the limiting deformation site.

The shear stresses changed their magnitude in relation to the transient process with a grip angle of 0.077 radians. The limits of change of shear stresses, Fig. 7, are 0.0...0.376, shear stresses, Fig. 4, 0.0...0.204. With the increase of the grip angle, the shear stresses responded by increasing. The convexity of the shear stress diagram with an increase in the form factor, for zero abscissa, within the limits of 0.201; 0.248; 0.285; 0.289; 0.241, increased in relation to the grip angle of 0.077 radians within the limits of 0.107; 0.121; 0.135; 0.154; 0.160; 0.149.

Changes in shear stresses characterize the processes of self-regulation of oppositely directed friction forces and normal pressure in the lagging zone. When rolling tall strips, i.e., for the first three shape factor curves, no reduction in contact stresses in the lag zone is observed with increasing grip angle, and there are no zones where the ultimate deformation site can be reached. Indeed, the maximum normal stress values for the three lower curves show an upward trend to 2.215. Moreover, in the lag zone, for these same curves, an increase from 1.239 to 1.614, rather than a decrease, occurs within the horizontal axis – 0.2. In the same series, but when rolling thin strips at factors of 8.61 and 11.07, a decrease in specific pressures within the lag zone is observed within the range of 1.496…1.247, indicating the presence of tensile stresses. The presented model of stressed state changes indicates the possibility of a transient process with an increase in the grip angle of 0.129 radians. There are zones of attainability of the limiting deformation site for thin strips, i.e., the effect is confirmed with an increase in the grip angle.

The next feature of the considered transition zone of deformation is the increase of tensile stress with the growth of the angle of capture. This increase is designated by the magnitude of the decrease in normal contact stresses in the lagging zone with the equality of other indices of the compared processes. The indices of the transient process shown in Fig. 4, 7 are compared. The lagging zone is selected for thin strips with the same value of the abscissa axis equal to – 0.2, with the same form factor of 8.61 and 11.07. For Fig. 4, on one horizontal axis – 0.2, the obtained stresses for the form factor of 8.61 and 11.07 are 1.485 and 1.474, respectively. For Fig. 7, on one horizontal axis – 0.2, the stresses for the form factor of 8.61 and 11.07 are 1.496 and 1.247, respectively. The difference within one figure gives the stress difference between the diagrams of adjacent form factor values, which must be compared:

$$1.496 - 1.247 = 0.249;\ 1.485 - 1.474 = 0.011.$$

The first difference relates to Fig. 7, with a larger grip angle, and the second to Fig. 4, with a smaller grip angle. The deflections are different: 0.249 and 0.011. The deflections are greater where the grip angles are larger, and therefore where the tensile stresses are greater.

Tensile stresses increase with increasing friction coefficient and with increasing grip angle, but at different rates. It should be noted that if the forces involved in generating the back tension change in magnitude, the tensile stresses from their interaction increase in accordance with the process accompanying this increase. This can be either a capture due to frictional forces or reverse metal flow due to normal extrusion pressure.

In summary: when implementing the process with an increased grip angle of 0.129 radians, it is shown that, for a given ratio of grip angle and friction coefficient, a transient process is possible, combining elements of a transient process and elements of a stable rolling process. The impact of tensile stresses on the rolling of tall strips is limited. Tensile stresses have a decisive effect on the rolling of thin and medium strips, manifesting themselves in the zones where the ultimate deformation site is reached or in the effect of reducing the force load.

Fig. 8 shows the contact stress diagrams for a grip angle of 0.129 radians and a friction coefficient of 0.251, which corresponds to a friction coefficient to grip angle ratio of 1.95, with a full-fledged lead zone.

A steady increase in maximum normal stresses is noted with increasing deformation site shape factor within the ranges of 1.409; 2.067; 2.824; 4.249; 5.308.

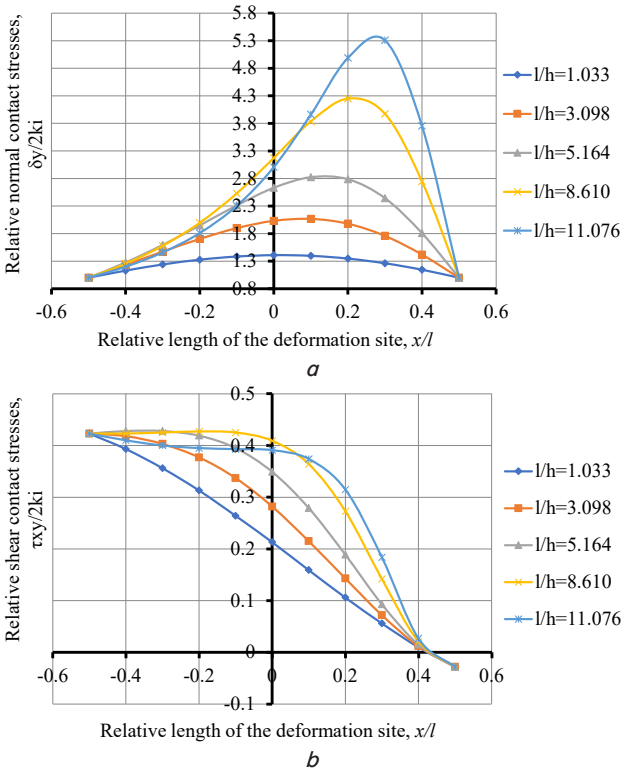

Fig. 8. Distribution of contact stresses along the deformation site during metal gripping by rolls under the conditions of the determining process at $l / h = 1.033...11.07$; $f = 0.251$; $\alpha = 0.129$: *a* – distribution of normal stresses; *b* – distribution of shear stresses

The shear stress variation limits for all shape factors are the same, within the range of –0.028…0.423, which are greater than the shear stresses at a grip angle of 0.077 (–0.025…0.233), determining the presence of a lead zone. There are significant differences in the curves determined by the convexity of the shear stress diagrams in the lag zone. Moreover, the parameters characterizing their magnitude depend primarily on the shape factor and are, for a zero abscissa, within the ranges of 0.213; 0.282; 0.349; 0.409; 0.391. In this list, the last value belongs to the curve that drops below the previous one with a shape factor of 8.61, Fig. 8, which is explained by the increasing effect of the tensile force in the lag zone. A distinctive feature of this process is the response of the force characteristics of the lag zone to an increase in the grip angle to 0.129, which is reflected in the increased concavity of the normal stress diagrams during the rolling of thin-walled strips.

Table 3 gives contact normal stress data in the lag zone for detailed analysis.

In Table 1, it was for these shape factors that minor deflections in the diagrams were already present in the lagging zone, indicating the sensitivity of thin-walled rolled products to the action of even minor tensile stresses. From Table 3 it follows that in the lagging zone, at a given grip angle, the stresses vary differently depending on the shape factor. Up to the factor value of 8.61, an increase in all contact stresses is indicated depending on the shape factor. For the abscissa of –0.3, starting from 8.61, a decrease in stresses occurs within

the range of 1.578; 1.459. The same trend is observed for the abscissa of –0.4, only within the range of 1.255; 1.200. A decrease in stresses also occurs for the abscissa of –0.1, up to a value of 2.304. The same correspondence of the data is confirmed by the diagrams in Fig. 5.

Table 3

Comparative data on relative normal contact stresses in the lag zone of the determining process at $\alpha = 0.129$ rad

Relative length in the lagging zone, x / l	Deformation site shape factor, l / h				
	1.033	3.098	5.164	8.61	11.07
	Relative normal contact stresses, $\sigma_y / 2k_i$				
–0.1	1.384	1.900	2.312	2.529	2.304
–0.2	1.327	1.704	1.949	1.996	1.810
–0.3	1.240	1.474	1.595	1.578	1.459
–0.4	1.129	1.234	1.,277	1.255	1.200
–0.5	1	1	1	1	1

Moreover, all rolling processes, represented by a ratio of the friction coefficient to the grip angle of 1.95, correspond to the realization of a stable grip of the metal by the rolls and the process itself.

This information boils down to one thing: the combined effect of the grip angle and the friction coefficient is the intensifying factor.

With an increase in the grip angle (reduction), contact stresses increase [1], and the friction coefficient acts in the same direction.

Table 4 gives relative values of the maximum normal stresses for two transient processes at grip angles of 0.077 and 0.129, a form factor of 11.07, and friction coefficients of 0.150 and 0.251, respectively.

The stress values at the exit of the deformation site, for both grip angles, are distinguished by high stress values at the entrance to the deformation site. In this case, before the abscissa –0.1, stresses with greater compression correspond to greater stresses, after the abscissa –0.1 the stressed state changes to the opposite.

Increasing the grip angle leads to a redistribution of the metal's stressed state along the deformation site.

Comparing the results of the processes shown in Fig. 5, 8, it was concluded that a stable rolling process occurs at different friction coefficients (from 0.150 to 0.251) for different grip angles. There was no decrease in the curve concavity below the minimum value (less than unity). Plastic deformation was present in the lag zone, forming a two-zone deformation site. With this ratio of process parameters, partial suppression of the zeroing tensile factors in the lag zone is evident. On the one hand, departure from the minimum stability process was evident due to an increase in the friction coefficient, while on the other hand, zones where the ultimate deformation site can be reached appeared due to an increase in the grip angle.

However, the suppression of tensile stresses in the compression zone varies. At a minimum grip angle of 0.077 and a friction coefficient of 0.150, tensile stresses were virtually absent. In the next case, the grip angle (0.129) and friction coefficient (0.251) increased. However, the influence of the friction coefficient on suppressing tensile stresses in the lagging zone was insufficient to achieve zero lead, as was the case with a grip angle of 0.077 radians. The influence of the grip angle, but not the friction coefficient, on the stressed state parameters in this case was decisive, as the interaction of these factors led to a load reduction effect with increasing deformation loading.

When the friction coefficient and grip angle interacted together, their influence was the predominant factor affecting contact stresses along the deformation site. The following pattern is characteristic of the lagging zone: smaller angles and friction coefficients correspond to higher contact stresses, while larger angles and friction coefficients correspond to lower contact stresses. Returning to Fig. 5, 8, it is clear that a transition from the process of suppressing stretching in the lagging zone to a process of enhancing its influence is evident. A characteristic feature is the manifestation of a load reduction effect with increasing deformation loading.

Fig. 9 shows diagrams of the beyond-limit process of metal capture by rolls for different form factor values, a minimum friction coefficient of 0.05, and the maximum grip angle (in the scope of this study) of 0.168. The ratio of the friction coefficient to the grip angle is less than unity, equal to 0.298. This is greater than the similar ratios for the grip angle of 0.077, equal to 0.195, and less than for the grip angle of 0.129, equal to 0.388. Thus, we have another out-of-limit process of metal capture by rolls, confirmed by the new out-of-limit curves in Fig. 9.

A reduction in the number of curves was observed compared to the beyond-limit processes shown in Fig. 3, 6. The absence of beyond-limit curves with shape factors of 15.49; 11.07 and the addition of a curve with a shape factor of 8.61 confirms that the beyond-limit grip mode is characterized by even lower stability in the critical state of the new process.

The tendency for additional control actions from the lag zone is enhanced due to the emergence of new zones where the ultimate deformation site is attainable. For the thinnest strip, when examined with a shape factor of 5.164, a deflection of the diagram is observed below the strip with a shape factor of 1.033, which may indicate that the ultimate stability values have been reached for all types of loading. The process with the minimum friction coefficient and maximum grip angle can be explained by the action of rearward tension from the lag zone. As the grip angle increases, the effect of the buoyancy force from the deformation site increases. According to the law of action and reaction, the magnitude of the gripping frictional force increases, which is confirmed by an increase in shear stresses in the lag zone. Under the influence of increased opposing forces, the tensile force at the deformation site increases. The effect of rearward tension promotes the reverse flow of metal from the deformation site, which eliminates the causes of the lead zone, aggravating the process of beyond-limit gripping. Contact normal stresses in the lag zone decrease, which is recorded in the contact stress diagrams, Fig. 9. Another deflection appears in the shear stress diagram. It should be noted that in Fig. 6, the increase in tensile force is characterized by an increase in the gripping frictional force,

Table 4

Comparative data on the relative maximum normal contact stresses of two transient processes with grip angles of 0.077 and 0.129 rad

Grip angle, rad	Relative length of deformation site, x / l										
	0.5	0.4	0.3	0.2	0.1	0.0	–0.1	–0.2	–0.3	–0.4	–0.5
	Relative maximum normal contact stresses, $\sigma_y / 2k_i$										
0.077	1.00	2.075	2.939	3.334	3.261	2.898	2.429	1.972	1.578	1.256	1.00
0.129	1.00	3.754	5.308	4.989	3.961	3.008	2.304	1.810	1.459	1.200	1.00

and in this case, the tensile force increases due to an increase in the buoyant force of normal pressure. The contact pressure diagrams of the high bands, shape factors of 1.033; 3.098 and 5.164, also responded to the increase in the grip angle by rearranging themselves. The curves with shape factors of 5.164 and 3.098 swapped places. The lower curve (3.098) rose, while the upper curve (5.164) sank. Moreover, in the lagging zone, the latter curve sank below the 1.033 curve. Similar changes in the stressed state also occurred for shear stresses at a grip angle of 0.168 radians. The complex transformation of the stressed state toward deterioration of the roll gripping capacity at the maximum capture is confirmed by the two-component nature of the capture and the emergence of new regulating factors at the deformation site.

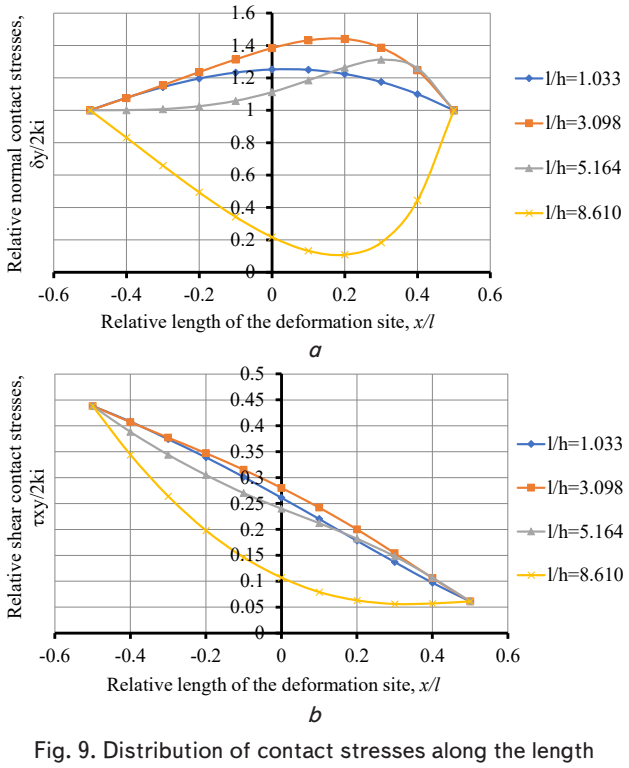

Fig. 9. Distribution of contact stresses along the length of the deformation site under conditions of extreme grip of metal by rolls at $l / h = 1.033...8.61$; $f = 0.05$; $\alpha = 0.168$: *a* – distribution of normal stresses; *b* – distribution of shear stresses

Fig. 10 shows a transient rolling process with a grip angle of 0.168 radians, but with a friction coefficient that allows for initial metal gripping by the rolls of 0.215 radians in the absence of a lead zone.

The ratio of the friction coefficient to the grip angle is 1.28, which is higher than the similar ratio of 1.19 for a grip angle of 0.129 radians. This process is defined as transient, as the design allows for the presence of a zero lead zone and metal gripping by the rolls. The process of buckling of the thinnest strip with a deformation site shape factor of 11.07 is considered. In the lagging zone, with a complete set of data on metal gripping by the rolls, an increased effect of the zeroing factor, i.e., strip stretching from the lagging zone, is evident. Fig. 10 shows that the diagram of the maximum value of the normal contact stress shape factor has an unacceptable concavity, less than unity. This indicates that the stresses at the deformation site are less than the yield strength, and plastic deformation is absent in this zone of the deformation site. The transition process occurs on the verge of loss of stability and is characterized by a maximum reduction in force action.

Let's analyze this process in more detail. With increasing shape factor, the maximum normal stresses increased to number 8.61 in the following sequence: 1.522; 2.248; 2.932; 3.383.

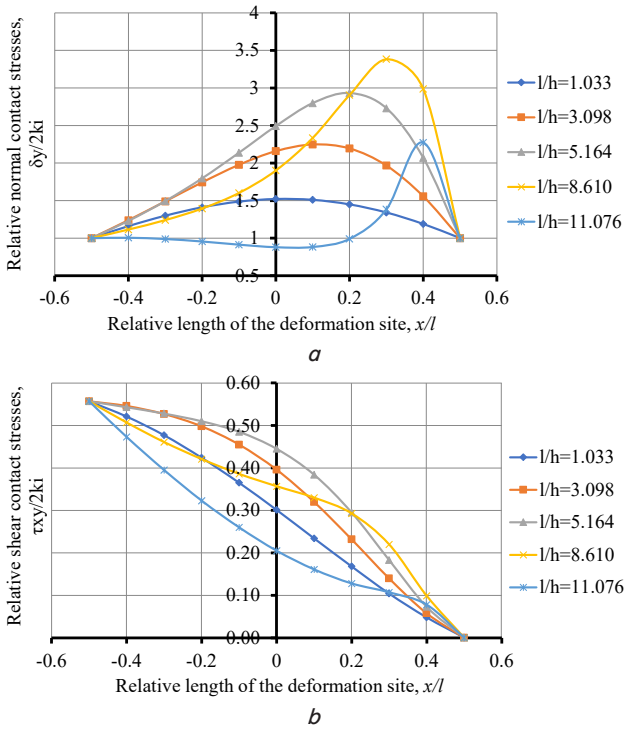

Fig. 10. Distribution of contact stresses along the deformation site during metal gripping by rolls under transient process conditions at $l / h = 1.033...11.07$; $f = 0.215$; $\alpha = 0.168$: *a* – distribution of normal stresses; *b* – distribution of shear stresses

This is determined by an increase in the friction coefficient to a value of 0.215, compared to a friction coefficient of 0.153 in the previous transient process, Fig. 7. The shear stresses also increase compared to the transient process, Fig. 8, respectively, from 0.0...0.376 to 0.0...0.557. This increase in shear stresses is explained by the interaction of oppositely directed gripping forces and normal pressures. As the grip of the metal by the rolls increases, pushing action of the normal force from the deformation site increases. According to the law of action and reaction, the gripping force of the metal by the rolls increases, which is confirmed by an increase in shear stresses. As a result of this interaction, the tensile force in the lagging zone increases to limit values. The tensile force suppresses frictional stress, and a restructuring of the stressed state occurs. Table 5 gives data on the transient process, at a maximum grip angle of 0.168 radians.

Table 5 demonstrates that loading the deformation site leads to a gradual shift in load reduction toward the lag zone for all shape factors.

This confirms the previously drawn conclusion that this primarily affects thin and extremely thin strips. Comparing the stress variation ranges for shape factors of 1.033 and 11.07, we obtain the following data: 1.16 to 1.522 and 0.880 to 2.373, respectively. The entire lag zone has variation ranges of 0.880 to 0.991. The stresses are outside the plastic deformation site. Stresses with a value of 11.07 have dropped below the stress diagram with a shape factor of 8.61 and are comparable to the stress diagram

with a value of 5.164. Furthermore, stresses in the lagging zone for a shape factor of 8.61 dropped below the 1.033 diagram, indicating the presence of a significant zone where the ultimate deformation site of the following curve can be reached.

Table 5

Comparative data on relative normal contact stresses of the transient process $\alpha = 0.168$ rad

Relative length of the deformation site, x / l	Deformation site shape factor, l / h				
	1.033	3.098	5.164	8.61	11.07
	Relative normal contact stresses, $\sigma_y / 2k_i$				
0.5	1	1	1	1	1
0.4	1.189	1.557	2.069	2.987	2.273
0.3	1.342	1.967	2.73	3.383	1.384
0.2	1.45	2.195	2.932	2.906	0.991
0.1	1.511	2.248	2.798	2.335	0.883
0	1.522	2.159	2.492	1.901	0.88
–0.1	1.487	1.977	2.137	1.602	0.914
–0.2	1.411	1.743	1.796	1.394	0.956
–0.3	1.299	1.49	1.493	1.24	0.989
–0.4	1.16	1.239	1.229	1.114	1.006
–0.5	1	1	1	1	1

The drop zone or increase in tensile stresses in the lagging zone can be quantified, as this was done relative to a grip angle of 0.129 radians. For the same shape factor parameters and the *x*-axis, –0.2, a sample was taken for a grip angle of 0.168 radians, yielding 1.394 and 0.956, respectively. The difference between these values is then 0.438, which is significantly greater for the same parameters but with a grip angle of 0.129 radians, equaling 0.249. The tensile stress values increased exponentially. Consequently, such an increase in tensile stresses facilitates the process reaching the ultimate deformation site more quickly, i.e., loss of stability and slippage of the strip in the rolls.

The curves of the shape factor diagrams of 1.033...5.164 (strips of large and medium thickness) did not respond to the attainability zone.

A transient rolling process has been considered, with the stressed state zeroing, under conditions of increasing stretching in the lag zone. This provides a striking example of confirmation of the effect of plastic deformation and a decrease in rolling force under maximum deformation loading. However, this process does not have a lead zone. This analysis reveals that the represented transient process meets all the requirements that a process within a limiting deformation site must meet [1].

The above studies demonstrate the implementation of a process with a single-zone deformation site, at the limit of its stability: a process within which the effect of plastic deformation is determined. For the possibility of its optimization, the inverse problem is of interest, i.e., suppression of the force-regulating effect from the lag zone under conditions of increasing gripping forces at the deformation site. In Fig. 5, 8, for the determining modes, the minimal impact of tensile stresses on the parameters of the compression zone is shown. The question arises about the impact of tensile stresses on the process parameters at the maximum grip angle.

Fig. 11 shows the metal gripping by rolls with the following process parameters: grip angle of 0.168 radians; friction coefficient of 0.327, in the presence of a leading zone. The ratio of the friction coefficient to the grip angle is 1.95, which is similar to the same ratio for a grip angle of 0.129 radians.

It is known that contact stresses also increase with an increase in the form factor. This pattern is observed for the first three processes with numbers 1.033; 3.098; 5.164 (high and medium-height strips) and the maximum stresses of strips with form factors of 8.61; 11.07 (thin strips). No loss of process stability is observed. However, the last two curves, at maximum specific pressures, have dips in the contact stress diagrams in the lagging zone. This leads to a sharp decrease in rolling force, relative to the diagrams with a lower form factor. Tensile stresses from the lag zone influence the deformation site. As Fig. 11 shows, increasing the friction coefficient does not eliminate this effect, but deflections in the diagrams smaller than unity do, indicating the presence of plastic deformation in the lag zone. Tensile stresses in the lag zone are partially suppressed, and stable rolling is achieved.

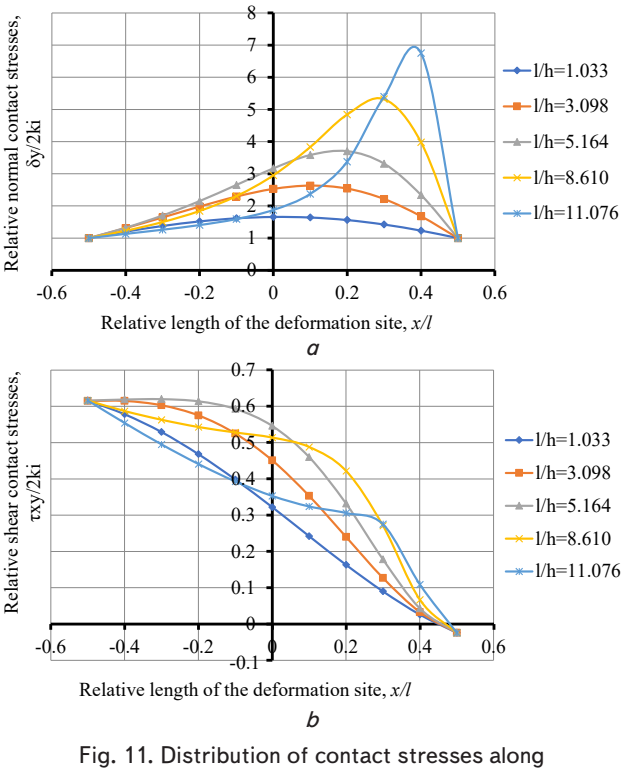

Fig. 11. Distribution of contact stresses along the deformation site during metal gripping by rolls under the conditions of the determining process at $l / h = 1.033...11.07$; $f = 0.327$; $\alpha = 0.168$: *a* – distribution of normal stresses; *b* – distribution of shear stresses

Similar patterns of reduction in the diagrams also occur for shear stresses, only relative to the inclined line, with a shape factor of 1.033. The shear stress ranges from –0.024 to 0.616 at a grip angle of 0.168 radians. This range is greater than that for a grip angle of 0.129 radians, which is –0.028 to 0.423. Moreover, the shear stress in the lead zone with greater compression (–0.024) is less than in the lead zone with less compression (–0.028). This is explained by the greater rear tension, which reduces the size of the lead zone, thereby creating conditions for reducing the shear contact stresses at the deformation site.

The maximum shear stress at the entrance to the deformation site, 0.616, is determined by the magnitude of the compression. This is confirmed by the stress distribution

depending on the grip angle in the determining processes involving the lead zone (Fig. 6, 9, 12). We have 0.077–0.233; 0.129–0.423; 0.168–0.616.

The change in normal stresses is more complex. Table 6 gives normal contact stress values for the determining process, with partial suppression of tensile stresses in the lagging zone.

Table 6

Comparative data on relative normal contact stresses of the determining process, $\alpha = 0.168$ rad

Relative length of the deformation site, x / l	Deformation site shape factor, l / h				
	1.033	3.098	5.164	8.61	11.07
	Relative normal contact stresses, $\sigma_y / 2k_i$				
0.5	1	1	1	1	1
0,4	1.232	1.679	2.34	3.981	6.751
0.3	1.423	2.217	3.313	5.32	5.401
0.2	1.563	2.541	3.701	4.842	3.374
0.1	1.642	2,634	3.581	3,831	2.374
0	1.66	2.531	3.167	2.95	1.874
–0.1	1.617	2.293	2.652	2.305	1.591
–0.2	1.52	1.981	2.149	1.842	1.404
–0.3	1.378	1.643	1.703	1.499	1.26
–0.4	1.201	1.311	1.322	1.228	1.131
–0.5	1	1	1	1	1

All parameters in Table 6 are greater than those in Table 5, which is explained by the influence of a higher friction coefficient of 0.327 and a grip angle of 0.168 radians. There are no subsidence of the maximum contact stress diagrams in comparison with Table 5. A general pattern of decreasing force load on the release zone is noted, starting with a shape factor of 8.61, with regard to the lagging zone. At the same time, there are no data on relative normal stresses less than unity, this is especially true for thin strips with a shape factor of 11.07. For this shape factor, the following loading parameters along the release zone length are valid: 1.0; 6.751; 5.401; 3.374; 2.374; 1.874; 1.591; 1.404; 1.260; 1.131; 1.0. Therefore, in contrast to Table 5, plastic deformation occurs at all points without the deformation site, meaning the rolling process is stable. This is a characteristic of this process, as is the case for the processes shown in Fig. 5, 8. In this case, a shift away from rolling with the limiting deformation site, as indicated in Fig. 10 and Table 5, toward increasing the stability of the plastic deformation regime has been identified.

If normal stresses are considered as a whole, they are characterized by complex changes and are not unambiguous.

There is an increase in the stressed state for the relative length indices of 0.4 and 0.3, respectively 1.232; 1.679; 2.340; 3.981; 6.751 and 1.423; 2.217; 3.313; 5.320; 5.401 in accordance with the data in Fig. 2. For the abscissas of 0.2 and 0.1, there is a decrease in stresses towards smaller thicknesses of the deformation site and a transition of curves 11.07 and 8.61 to the zone of attainability of the limiting deformation site. In this case, the transition efficiency is higher for the diagram with the shape factor of 11.07, in comparison with the diagram, 8.61. This is confirmed by the curves in the region of the lag zones and the diagrams in Fig. 11. Unlike the transient process (Fig. 10), no loss of stability was observed in processes with an advance zone. However, the influence of tensile stress is decisive here.

At the maximum grip angle, when the gripping capabilities of the rolling process are minimal (Fig. 10), processes occur in which the effect of tensile forces is partially suppressed, and the deformation site transitions from a single-zone to a two-zone zone. There are no concavities in the diagrams with no plastic deformation. This is due to increased contact frictional forces. In this case, the tensile forces are neutralized by the increased contact frictional forces.

As a result, signs of stabilization appear for the determining processes shown in Fig. 5, 8. Process stability and the roll gripping capacity are restored. This is particularly evident in the steady increase in maximum normal stresses for all form factors. Accordingly, tensile forces are reduced, creating conditions for plastic deformation in the lag zone. Excessive deflections at the deformation site are eliminated.

However, despite all this, stresses are reduced relative to processes with a lower form factor, meaning that zones within which the ultimate deformation site can be reached remain. These zones, at a given gripping angle, are very significant. These zones do not completely disappear with increasing friction coefficients, so further compensation requires increasing friction coefficients. Therefore, the question arises as to what limits the process of increasing friction stresses should be carried out, taking into account the attainability of the ultimate deformation site. A key feature of this process, from the standpoint of optimizing the plastic deformation effect, is the rolling conditions that are close to process stability. This introduces significant uncertainty into the solution to this problem.

To solve this problem, it is necessary to understand the definition of process certainty or stability, or a process without roll slippage. In this case, with the maximum grip angle, the process is destabilized in terms of the metal gripping by the rolls. A process suppressing the tensile effect on the plastic deformation site has been identified. The final example demonstrates that the process exists, and that parameters for this process exist that indicate the limits of increasing the metal gripping by the rolls, i.e., process stabilization.

5. 3. Evaluating the reliability of results based on investigating the stressed state of metal under the influence of multiparametric factors

According to expression (28), Fig. 2 shows the stress distribution along the deformation site length as a function of the shape factor l / h. The relative normal and shear stresses are denoted as $\sigma_y / 2k$ and $\tau_y / 2k$, and the relative length of the deformation site is x / l.

Fig. 12 shows experimental contact stress diagrams during rolling, obtained using point mass measurements in [1]. First, the qualitative indicators of the experimental and calculated data are compared. The compared diagrams demonstrate that with an increase in the shape factor, the stressed state of the plastic medium increases. The shape of the stress diagrams also changes. At the minimum value of the shape factor, the contact stress diagram has a symmetrical shape (shape factor 0.9) and a virtually uniform distribution along the deformation site length.

As the form factor increases, the loading asymmetry increases, and the maximum normal stress values shift toward the metal exiting the plastic flow zone. In the lag zone, at high form factor values, a concavity in the normal contact stress diagrams is visible on the entry side, indicating the presence of tensile longitudinal stresses in this zone (Fig. 1, 2, 12), consistent with the adopted physical model of the process. This demonstrates the comparability of the physical models for

calculated and experimental data. Regarding the tangential stresses, it is worth noting the sign change upon crossing the zero line, confirming the opposite nature of metal flow in the lag and lead zones.

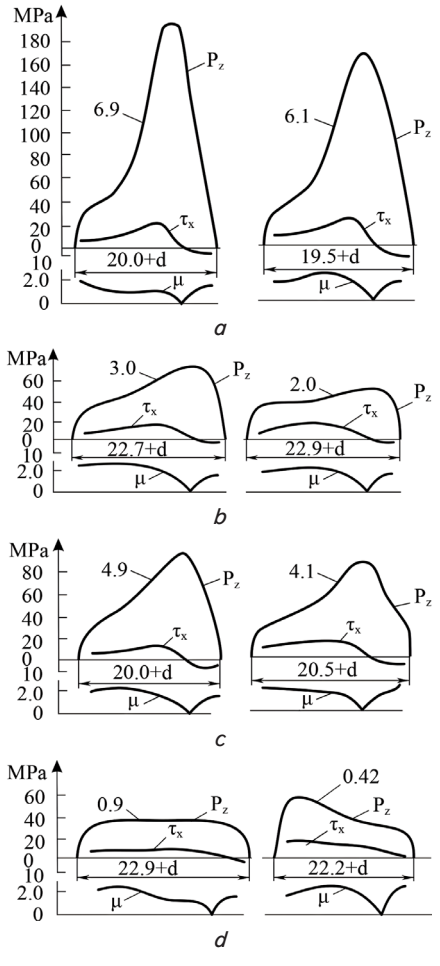

Fig. 12. Experimental data on the distribution of contact stresses depending on the shape factor l_D / h_{ave}: a – $l_D / h_{ave} = 6.9; 6.1$; b – $l_D / h_{ave} = 4.9; 4.1$; c – $l_D / h_{ave} = 3.0; 2.0$; d – $l_D / h_{ave} = 0.9; 042$; l_D – length of the deformation site; h_{ave} – average height

In early works on rolling theory [1], when the linear problem in plasticity theory was solved separately for the lag and lead zones, it was assumed that the specific contact stresses in the neutral section had a discontinuity at the transition from the lag to the lead zone. As can be seen from experimental and theoretical studies, such discontinuity in the transition zone at the neutral cross-section is absent, which enhances the reliability of the calculated data.

When comparing quantitative process characteristics, certain difficulties arise due to the way the results are represented. The calculated value diagrams are shown in relative units, while the experimental data are represented in absolute units (MPa). However, it is also possible to represent the experimental data in relative terms. If 40 MPa is taken as the base value, which is not the hardened yield strength, then for a shape factor of 6.9, the back-pressure factor will be equal to 4.625 (Fig. 12).

The closest calculated shape factor of 8.61 to a shape factor of 6.9 indicates a back-up coefficient of 4.1. At first glance, the result doesn't seem to align with the calculated data, as a higher shape factor should correspond to a higher back-up coefficient, not vice versa. However, according to [1], the back-up coefficient is significantly affected by compression, which was significant in experimental studies. By equating these factors and using a mathematical model of the process, we were able to recalculate the result, which was within 3...5% for all experimental and calculated data.

It can therefore be concluded that the calculated and experimental data, adjusted to the same initial values, demonstrate qualitative comparability and quantitative convergence within 3...5%.

The reported reliability result strengthens the justification for the adopted physical model of the process, characterized by the presence of tensile longitudinal stresses in the lagging zone, which decisively influence the conditions of metal gripping by the rolls and the stability of the rolling process. The obtained result, which allows one to solve complex theoretical and applied problems, must be tested in a specific manner, i.e., its validity must be determined. For complex problems, it is not always possible to implement an experiment due to the complexity of the equipment, the technology, or even the impossibility of implementing it altogether. In such cases, an attempt is made to simplify the obtained result. The mathematical model is reduced to a specific case, and an experiment or process simulation is implemented for this solution. If the result of the specific model confirms the generally accepted solution pattern, then in many cases this is sufficient to confirm its validity and further use in testing more complex problems.

In [1], the effect of plastic deformation was identified: under certain conditions, this is a decrease in force loading with an increase in deformation impact. Our study examines these determining conditions for metal gripping by rolls and the stability of the rolling process. Since implementing an experiment for contact stresses during rolling under multiparameter impacts presents a complex technical and technological challenge, finite element modeling of the hot rolling process of blanks in smooth-barrel rolls was conducted in the DEFORM program to confirm the reliability of the results.

To simplify the assessment of the reliability of results, generalized force characteristics of the loading were used rather than contact stresses. This necessitated the conversion of stresses into forces using stressed state coefficients [1].

The calculated values were based on the mathematical modeling results given in Tables 3, 5 in [1]. In our study, the basic data from those tables are given in Tables 7, 8. The following data, given in Tables 7, 8, are considered for different friction coefficients at $l / h = 11.07$; $\alpha = 0.077$; $f = 0.5...0.05$; and with different grip angles at $l / h = 11.04$; $\alpha = 0.077$; $\alpha = 0.129$; $\alpha = 0.168$; $f = 0.4$.

Table 7 gives the response of the mathematical model to changes in the external force, through the friction coefficient, on the contact stresses of the deformation site.

Table 7

Results of investigating the stressed state of the strip depending on the friction coefficient at $l / h = 11.07$; $\alpha = 0.077$ rad; $f = 0.5...0.05$ [1]

Coefficient of friction f	0.5	0.4	0.3	0.2	0.1	0.05
Maximum stress coefficient n_σ	7.4	6.9	5.7	4.1	2.5	1.6
Average stress coefficient n_σ	4.0	3.8	3.3	2.6	1.8	1.3

Table 8

Results of investigating the stressed state of the strip depending on the grip angle at $l / h = 11.07$; $f = 0.4$ [1]

Grip angle α, rad	0.77	0.129	0.168
Maximum stress coefficient n_σ	6.9	8.1	9.4
Average stress coefficient n_σ	3.8	3.9	3.3

Table 8 gives the response of the mathematical model to changes in the external force, through the grip angle, on the contact stresses of the deformation site. It should be noted that the mathematical model responds to the effect of plastic deformation. Indeed, with an increase in the grip angle, the compression increases, while a decrease in the force load is observed. Therefore, the maximum deformation effects, $\alpha = 0.168$, correspond to the minimum force loads, $n_\sigma = 3.3$, Table 8.

It should be noted that in Tables 7, 8, the average stressed state coefficient is a relatively integral characteristic of the force loading of the deformation site.

Classical formulas [3] were used to calculate the rolling force:

$$P = p_{ave}F; \tag{29}$$

$$p_{ave} = \beta\sigma_i n_\sigma;\ \beta\sigma_i = 2k; \tag{30}$$

$$F = \sqrt{R\Delta h}\cdot b_{ave}, \tag{31}$$

where n_σ is the average stressed state coefficient, taken from Tables 7, 8. Taking into account that in 2D modeling (flat state) the width of the workpiece is taken to be equal to one, and the value $k = 10$ MPa for technical lead, then formula (29) takes the following form

$$P = 20n_\sigma\sqrt{R\Delta h}\cdot b_{ave}. \tag{32}$$

The initial data for Experiment 1 (Tables 9, 10) and Experiment 2 (Tables 11, 12) were determined from Tables 7, 8.

Table 9 gives the workpiece thicknesses and roll radii for Experiment 1, i.e., for different friction coefficient values.

Table 9

Initial conditions for Experiment 1

l / h	Grip angle α, rad	Initial strip thickness h_0, mm	Final strip thickness h_1, mm	Roll radius R, mm	Coefficient of friction f
11.07	0.077	5	2	500	0.5
					0.4
					0.3
					0.2
					0.1
					0.05

To convert stresses into forces, expressions (29) to (32) were used, which applied the stressed state coefficients given in Table 10. Table 10 gives the calculated maximum and average values of the stressed state coefficients for Experiment 1.

Table 10

Values of the stress coefficient for Experiment 1

Coefficient of friction f	Maximum value of the stress state coefficient $n_{\sigma\_\max}$	Average value of the stress coefficient n_{σ_ave}
0.5	7.4	4.0
0.4	6.9	3.8
0.3	5.7	3.3
0.2	4.1	2.6
0.1	2.5	1.8
0.05	1.6	1.3

In accordance with Tables 9, 11 gives values of the workpiece thickness and the roll radius for Experiment 2, i.e., for different values of the grip angle.

Table 11

Initial conditions for Experiment 2

l / h	Grip angle α, rad	Initial strip thickness h_0, mm	Final strip thickness h_1, mm	Roll radius R, mm	Coefficient of friction f
11.07	0.077	5	2	500	0.4
	0.129	10.98	1.83	550	
	0.168	19.038	0.692	650	

In accordance with Tables 10, 12 gives the calculated maximum and average values of the stressed state coefficients for Experiment 2.

Table 12

Values of the stress coefficient for Experiment 2

Grip angle α, rad	Maximum stress coefficient $n_{\sigma\_\max}$	Average stress coefficient n_{σ_ave}
0.077	6.9	3.8
0.129	8.1	3.9
0.168	9.4	3.3

In the framework of the 1st experiment, Tables 9, 10, the following values of friction coefficients were used for analysis: 0.5; 0.3; 0.2; 0.1; 0.05. The minimum grip angle is $\alpha = 0.077$, form factor – $l / h = 11.07$. The results of finite element modeling in the DEFORM program are shown in Fig. 13.

Using expressions (29) to (32), calculated data were obtained for determining not the relative process parameters but specific force characteristics (Table 13). In addition to the calculated values of the integral force characteristics, Table 13 gives the force characteristics for simulation results.

Table 13 demonstrates that high convergence of the calculation and modeling results is maintained for friction coefficient values up to 0.1. However, for low friction coefficient values of 0.1 and 0.05, the error increases significantly to 12%. This can be explained by the influence of the zone of attainability of the limiting deformation site and the possibility of loss of rolling stability, i.e., metal slippage in the rolls.

In the second experiment (Tables 11, 12), the following values of grip angles were used for analysis: 0.077; 0.129; 0.168. Friction coefficient – 0.4; form factor $l / h = 11.07$. The results of finite element modeling in the DEFORM program are shown in Fig. 14.

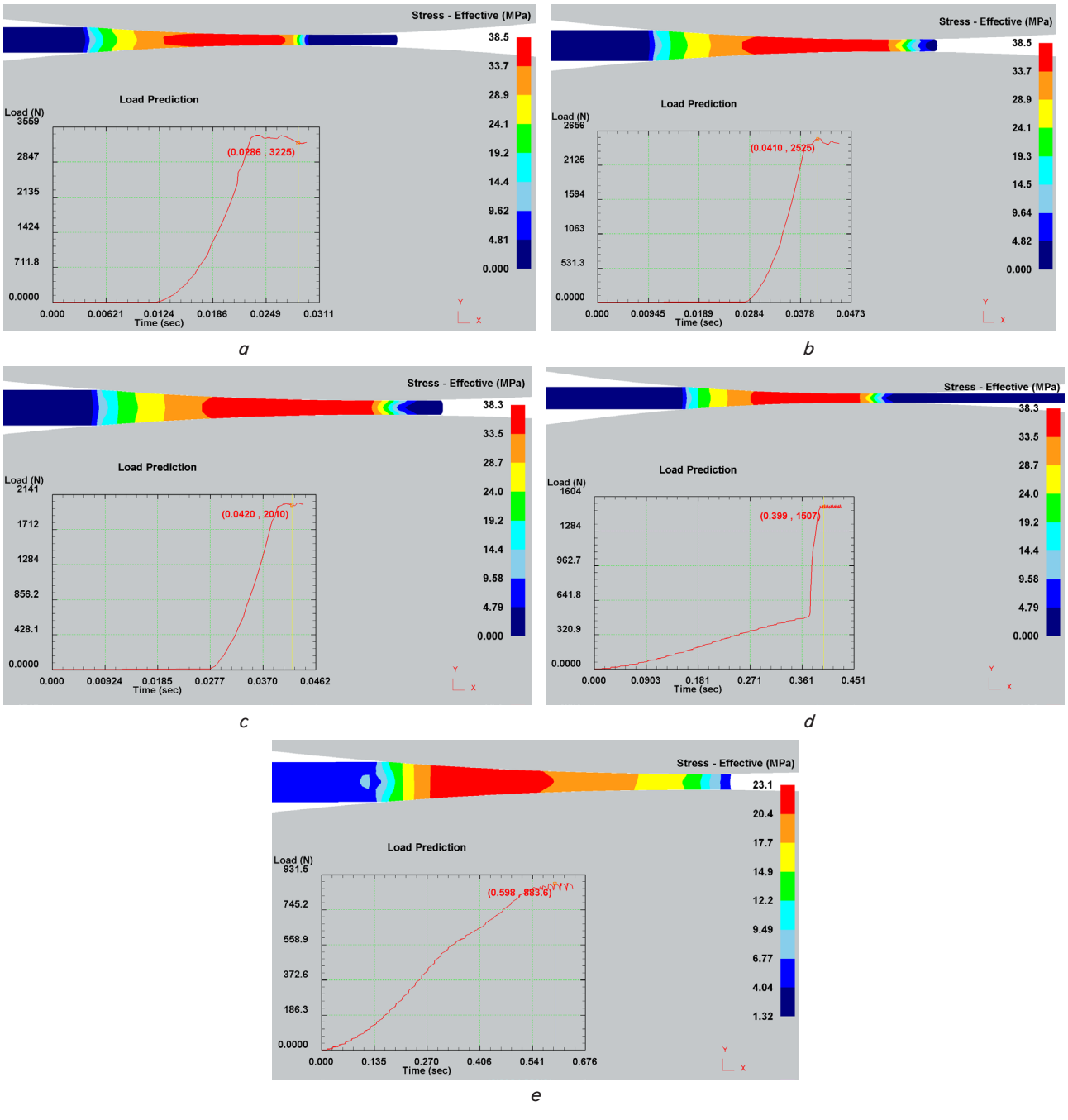

Fig. 13. Simulation results for different values of the friction coefficient:
a – $f = 0.5$; *b* – $f = 0.3$; *c* – $f = 0.2$; *d* – $f = 0.1$; *e* – $f = 0.05$

Table 13

Summary values of rolling forces for the 1st experiment

Coefficient of friction f	Calculated value of rolling force, P_{calc}, N	The value of rolling force in simulation, P_{sim}, N	Error, %
0.5	3098	3225	4.1
0.4	2943	2940	0.1
0.3	2556	2525	1.2
0.2	2013	2010	0.15
0,1	1394	1507	8.1
0.05	1006	884	12.1

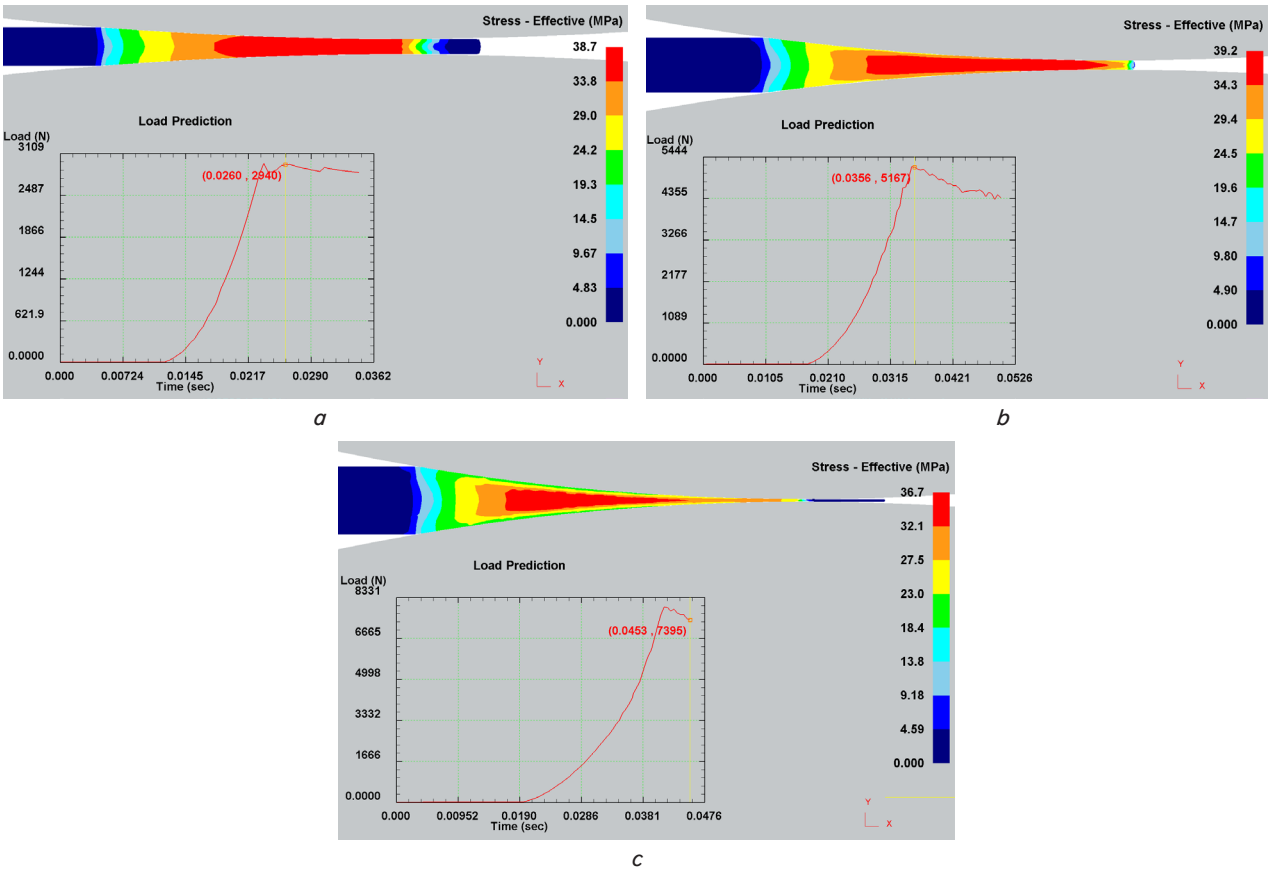

Fig. 14. Simulation results: *a* – $\alpha = 0.077$; *b* – $\alpha = 0.129$; *c* – $\alpha = 0.168$

Using the same expressions (29) to (32), data were obtained to determine the force parameters of the process in Experiment 2, Table 14. The difference between the calculated values and those obtained through modeling was within 0.1–6.6%. These are indicators of high convergence of the results. Moreover, the dependence of the stressed state at the deformation site on the next influencing factor, the grip angle or compression along the strip height, is emphasized.

Table 14

Summary values of rolling forces for Experiment 2

l / h	Grip angle α, rad	Calculated value of rolling force, P_{calc}, N	The value of rolling force in simulation, P_{sim}, N	Error, %
11.07	0.077	2943	2940	0.1
	0.129	5533	5167	6.6
	0.168	7207	7395	2.6

The following conclusions were drawn from the data in Tables 13, 14: the values of the integral characteristics of the force loading (rolling forces), obtained by calculation and modeling, have high convergence due to the small difference between them for all the cases under consideration under conditions of varying contact friction and compression.

It should also be noted that the process modeling responded to changes in the rolling forces due to the effect of plastic deformation.

Our detailed studies on the reliability of results from the physical and mathematical models in [1] and this research allow us to confirm that the physical model and the current studies of the roll gripping capacity and the stability of the rolling process are reliable in accordance with the reliability indicators presented above.

6. Discussion of results based on investigating the stressed state of metal under the influence of multiparametric factors

The mechanism of roll gripping ability and rolling at the process stability limit has been determined. Based on it, a physical and mathematical model of the process was built, represented by expression (28), based on the solution to a closed problem in plasticity theory. The method of argument functions of a complex variable was used. The main factor in this mechanism was a new feature that had not previously been considered when determining roll gripping ability: the effect of tensile stresses from the lagging zone on the rolling force parameters. Mathematical model (28) responded to this feature of the process.

The roll gripping ability and the rolling process were assessed using visual diagrams of normal and shear contact stresses constructed based on the mathematical model built.

Three loading regimes were considered for each grip angle: extreme, transient, and determining. The extreme process is shown in Fig. 3, 6, 9, and Table 2, for grip angles of 0.077, 0.129, 0.168 rad; the transient process is shown in Fig. 4, 7, 10, Table 5, for grip angles of 0.077, 0.129, 0.168 rad; the determining process is shown in Fig. 5, 8, 11, Tables 1, 3, 4, 6, for grip angles of 0.077, 0.129, 0.168.

The nature and magnitude of the diagrams for all three processes differ fundamentally. Stable rolling occurs in the

determining process. The normal stress diagram, although somewhat concave, does not intersect the limiting ordinate equal to unity, within which plastic deformation is absent. Shear stresses define a two-zone deformation site, within which a leading zone occurs. These factors ensure stable grip of the metal by the rolls and a stable rolling process.

The beyond-limit process is characterized by the absence of gripping ability of the rolls, and thus the absence of rolling as such. This is reinforced by the characteristic features and magnitude of the normal and shear stress diagrams. Normal stresses throughout the deformation site have a sharply concave diagram significantly smaller than the limiting ordinate equal to unity. There is a complete absence of plastic deformation along the entire length of the deformation site. Shear stresses form a single-zone deformation site, not intersecting the zero line and not changing their sign. There is a complete absence of the leading zone. These factors, including the absence of metal grip by the rolls and the rolling process, are confirmed by diagrams of both normal and shear stresses. However, this construction has its own peculiarities. There are curves in which, according to the normal stress diagrams, plastic deformation occurs (thick rolled product), but the shear stresses show that they do not change sign, and there is no lead zone. Such an intermediate nature of force loading can occur [1] when negative lead is realized. Remarkably, the mathematical model responds to such features of metal grip by the rolls. Thus, an unstable metal grip process is allowed in the absence of a lead zone.

The transient rolling process is of particular interest when applied to rolling processes near the point of loss of stability. In this case, variations in the absence of a zero-lead zone are possible. Plastic deformation occurs, as evidenced by the normal contact stress diagram, whose values lie above the limiting ordinate equal to unity. In this case, the retracting frictional force is greater than the expulsive force, in the absence of a lead zone. This is made possible by the action of tensile stresses from the lagging zone. Tensile stresses from the entrance to the deformation site reduce the extent of the lead zone, which facilitates its disappearance. Thus, the transient process combines the features of a beyond-limit process and a determining process, which contrasts with two-zone deformation site technologies [9, 13]. In this case, the normal and shear contact stress diagrams indicate that the zero-lead zone corresponds to the realization of plastic deformation. If plastic deformation was present during the gripping of the metal by the rolls, then gripping has occurred. Therefore, the use of a mechanism with a zero-lead zone characterizes the rolling process at the brink of loss of stability, which causes plastic deformation. This raises the prospect and necessity of devising a new technological process for a single-zone deformation site, with decreasing force loading and increasing deformation impact.

Technologically, maintaining the lead zone at zero is achieved by varying the friction coefficient and the grip angle. This requires determining the friction coefficient if the grip angle is known, assuming the numerator in expression (24) is zero. A special case for solving this problem is expression (27), which allows one to calculate the process with a lead zone equal to zero.

For further analysis and calculation of the zero lead zone, the following numerical relationships must be adhered to: for $\alpha = 0.077$, the ratio $f / \alpha = 1.10...1.95$; for $\alpha = 0.129$, the ratio $f / \alpha = 1.19...1.95$; for $\alpha = 0.168$, the ratio $f / \alpha = 1.28...1.95$.

The effects of plastic deformation are confirmed by experimental data on contact stress diagrams during rolling and by modeling the effect of plastic deformation under process conditions with varying contact friction and relative reduction.

A limitation of this approach is the lack of an analytical solution to the spatial problem of plasticity theory using the argument function method of a complex variable. Applying this solution in a production environment could improve the spatial results, including the effect of loading asymmetry on the parameters of the plastic deformation site, taking into account the characteristics of transverse metal flow.

Further advancement of our approach is envisaged by applying the obtained theoretical and experimental data to devising new rolling technologies with a single-zone deformation site, including, in the future, the development of a technology with severe plastic deformation.

7. Conclusions

1. A physical and mathematical model of the process has been built, characterizing the presence of longitudinal tensile stresses in the lag zone, which generate force loading in extreme, transient, and determining effects. Their characteristics are shown in the absence of grip, during a stable process, and for a process with a zero lead zone.

2. Our study has revealed a new single-zone deformation regime with minimal process stability. The zones of attainability of the limiting deformation site were determined, and the stability indices of transient regimes were defined: at $\alpha = 0.077$, the ratio $f / \alpha = 1.10...1.95$; at $\alpha = 0.129$, the ratio $f / \alpha = 1.19...1.95$; at $\alpha = 0.168$, the ratio $f / \alpha = 1.28...1.95$.

3. We have experimentally assessed the reliability of results by simulation when studying the stressed state of metal under the influence of multiparameter factors on the grip and stability of the rolling process. The error in the calculated stress values during the experimental comparison was within 3...5%; the error in the calculated values during the DEFORM simulation was 0.1...8.1% for friction and 0.1...6.6% for compression.

Conflicts of interest

The authors declare that they have no conflicts of interest in relation to the current study, including financial, personal, authorship, or any other, that could affect the study, as well as the results reported in this paper.

Funding

This study was funded by the Science Committee of the Ministry of Science and Higher Education of the Republic of Kazakhstan (topic No. AR 19678682 based on the contract for conducting scientific research work No. 232/23-25 dated August 23, 2023).

Data availability

The manuscript has associated data in the data warehouse.

Use of artificial intelligence

The authors confirm that they did not use artificial intelligence technologies when creating the current work.

References

1. Chigirinsky, V., Naizabekov, A., Lezhnev, S., Naumenko, O., Kuzmin, S. (2024). Determining the patterns of asymmetric interaction of plastic medium with counter-directional metal flow. Eastern-European Journal of Enterprise Technologies, 1 (7 (127)), 66–82. https://doi.org/10.15587/1729-4061.2024.293842
2. Chigirinsky, V., Naizabekov, A., Lezhnev, S., Kuzmin, S., Panin, E., Tolkushkin, A. et al. (2024). Effect of the limiting deformation zone under conditions of asymmetric loading during rolling of medium thickness strips. Journal of Chemical Technology and Metallurgy, 59 (4), 993–1002. https://doi.org/10.59957/jctm.v59.i4.2024.30
3. Chigurinski, V. V. (1999). The study of stressed and deformed metal state under conditions of nonuniform plastic medium flow. Metalurgija, 38 (1), 31–37.
4. Chigirinsky, V., Putnoki, A. (2017). Development of a dynamic model of transients in mechanical systems using argument-functions. Eastern-European Journal of Enterprise Technologies, 3 (7 (87)), 11–22. https://doi.org/10.15587/1729-4061.2017.101282
5. Chigirinsky, V., Naumenko, O. (2021). Advancing a generalized method for solving problems of continuum mechanics as applied to the Cartesian coordinate system. Eastern-European Journal of Enterprise Technologies, 5 (7 (113)), 14–24. https://doi.org/10.15587/1729-4061.2021.241287
6. Chigirinsky, V., Naizabekov, A., Lezhnev, S. (2021). Closed problem of plasticity theory. Journal of Chemical Technology and Metallurgy, 56 (4), 867–876. Available at: https://journal.uctm.edu/node/j2021-4/28_21-32p867-876.pdf
7. Chigirinsky, V., Naizabekov, A., Lezhnev, S., Kuzmin, S., Naumenko, O. (2022). Solving applied problems of elasticity theory in geomechanics using the method of argument functions of a complex variable. Eastern-European Journal of Enterprise Technologies, 5 (7 (119)), 105–113. https://doi.org/10.15587/1729-4061.2022.265673
8. Vasyliev, L., Malich, M., Vasyliev, D., Katan, V., Rizo, Z. (2023). Improving a technique to calculate strength of cylindrical rock samples in terms of uniaxial compression. Mining of Mineral Deposits, 17 (1), 43–50. https://doi.org/10.33271/mining17.01.043
9. Drahobetskyi, V. V., Shapoval, O. O., Shchepetov, V. V., Zahirniak, M. V., Lotous, V. V., Lehotkin, H. I. et al. (2017). Kerovani efekty plastychnoho deformuvannia zahotovok vyrobiv dlia metalurhiyi ta transportu. Kharkiv: "Drukarnia Madryd", 244. Available at: https://www.kdu.edu.ua/new/PHD_vid/KEPDZVMT.pdf
10. Dhinwal, S. S., Toth, L. S., Lapovok, R., Hodgson, P. D. (2019). Tailoring One-Pass Asymmetric Rolling of Extra Low Carbon Steel for Shear Texture and Recrystallization. Materials, 12 (12), 1935. https://doi.org/10.3390/ma12121935
11. Banerjee, A., Wylie, A., Da Silva, L. (2022). Near-Net Shape Manufacture of Ultra-High Strength Maraging Steel Using Flow Forming and Inertia Friction Welding: Experimental and Microstructural Characterization. Journal of Manufacturing Science and Engineering, 145 (2). https://doi.org/10.1115/1.4055519
12. Dhinwal, S. S., Toth, L. S., Hodgson, P. D., Haldar, A. (2018). Effects of Processing Conditions on Texture and Microstructure Evolution in Extra-Low Carbon Steel during Multi-Pass Asymmetric Rolling. Materials, 11 (8), 1327. https://doi.org/10.3390/ma11081327
13. Nadai, A. (1954). Theory of low and fracture of solids. IL Publ., New York.
14. Timoshenko, S. P., Goodier, J. N. (1952). Theory of Elasticity. Timoshenkoand Goodier. McGraw-Hill. New York 1951. 493 pp. 270 diagrams. 81s. net. (New Edition.). The Journal of the Royal Aeronautical Society, 56 (496), 308–308. https://doi.org/10.1017/s036839310012471x
15. Dorofeyev, O. A., Kovtun, V. V. (2019). Estimation of the Stress-Strain State of a Discrete Medium by a Plastic Flow Model. PROBLEMS OF TRIBOLOGY, 93 (3), 29–38. https://doi.org/10.31891/2079-1372-2019-93-3-29-38
16. El-Naaman, S. A., Nielsen, K. L., Niordson, C. F. (2019). An investigation of back stress formulations under cyclic loading. Mechanics of Materials, 130, 76–87. https://doi.org/10.1016/j.mechmat.2019.01.005
17. Lopez-Crespo, P., Camas, D., Antunes, F. V., Yates, J. R. (2018). A study of the evolution of crack tip plasticity along a crack front. Theoretical and Applied Fracture Mechanics, 98, 59–66. https://doi.org/10.1016/j.tafmec.2018.09.012
18. Li, J., Zhang, Z., Li, C. (2017). Elastic-plastic stress-strain calculation at notch root under monotonic, uniaxial and multiaxial loadings. Theoretical and Applied Fracture Mechanics, 92, 33–46. https://doi.org/10.1016/j.tafmec.2017.05.005
19. Pathak, H. (2017). Three-dimensional quasi-static fatigue crack growth analysis in functionally graded materials (FGMs) using coupled FE-XEFG approach. Theoretical and Applied Fracture Mechanics, 92, 59–75. https://doi.org/10.1016/j.tafmec.2017.05.010
20. Correia, J. A. F. O., Huffman, P. J., De Jesus, A. M. P., Cicero, S., Fernández-Canteli, A., Berto, F., Glinka, G. (2017). Unified two-stage fatigue methodology based on a probabilistic damage model applied to structural details. Theoretical and Applied Fracture Mechanics, 92, 252–265. https://doi.org/10.1016/j.tafmec.2017.09.004
21. Sneddon, I. N., Berry, D. S. (1958). The Classical Theory of Elasticity. Elasticity and Plasticity/Elastizität Und Plastizität, 1–126. https://doi.org/10.1007/978-3-642-45887-3_1
22. Hussein, N. S. (2014). Solution of a Problem Linear Plane Elasticity with Mixed Boundary Conditions by the Method of Boundary Integrals. Mathematical Problems in Engineering, 2014 (1). https://doi.org/10.1155/2014/323178
23. Yu, T., Xue, P. (2022). Introduction to Engineering Plasticity. Elsevier. https://doi.org/10.1016/c2021-0-00546-0
24. Muñoz, J. A., Avalos, M., Schell, N., Brokmeier, H. G., Bolmaro, R. E. (2021). Comparison of a low carbon steel processed by Cold Rolling (CR) and Asymmetrical Rolling (ASR): Heterogeneity in strain path, texture, microstructure and mechanical properties. Journal of Manufacturing Processes, 64, 557–575. https://doi.org/10.1016/j.jmapro.2021.02.017